BELPERAIN, SARAH, M.S. A Study of the Effect of Carbon Nanodots on Proinflammatory Cytokine TNF-α Induced Endothelial Dysfunction. (2020) Directed by Dr. Zhenquan Jia 50 pp.

Cardiovascular disease (CVD) has become an increasingly important topic in the field of medical research due to the steadily increasing rates of mortality caused by this disease [1]. With recent advancements in nanotechnology, a push for new, novel treatments for CVD utilizing these new materials has begun. Carbon Nanodots (CNDs), are a new form of nanoparticles that have been coveted due to the green synthesis method, biocompatibility, fluorescent capabilities and potential anti-antioxidant properties. With much research pouring into CNDs being used as bioimaging and drug delivery tools, little studies have been completed on their anti-inflammatory potential, especially in the cardiovascular system. Atherosclerosis begins initially by endothelial cell inflammation. The cause of this inflammation can come from many sources; one being tumor necrosis factor (TNF-α), which can not only trigger inflammation, but prolong its existence by causing a storm of pro-inflammatory cytokines. This study investigated the ability of CNDs to attenuate TNF-α induced inflammation in human microvascular endothelial cells (HMEC-1). Results show that CNDs reduce the expression of pro-inflammatory genes, mainly Interleukin-8 (IL-8), and Intercellular adhesion molecule-1 (ICAM), at the same time, increase heme oxygenase 1 (HO-1) gene expression. The uptake of CNDs by HMEC-1s was examined. Results from the studies involving channel blockers and endocytosis disruptors suggest that uptake takes place by endocytosis

A STUDY OF THE EFFECT OF CARBON NANODOTS ON PROINFLAMMATORY CYTOKINE TNF-α INDUCED ENDOTHELIAL DYSFUNCTION

by

Sarah Belperain

A Thesis Submitted to
the Faculty of The Graduate School at
The University of North Carolina at Greensboro
in Partial Fulfillment
of the Requirements for the Degree
Master of Science

Greensboro
2020

Approved by

_____
Committee Chair

APPROVAL PAGE

This thesis written by Sarah Belperain has been approved by the following committee of the Faculty of The Graduate School at The University of North Carolina at Greensboro.

Committee Chair _____

Committee Members _____

_____

_____
Date of Acceptance by Committee

_____
Date of Final Oral Examination

ACKNOWLEDGEMENTS

I would like to thank Dr. Zhenquan Jia for allowing me the opportunity to work within his lab, along with all the members in the Jia lab. I also would like to thank my committee members, Dr. Paul Steimle and Dr. Ramji Bhandari for their contribution and guidance on this project. And a thank you to my family, friends, and the Biology Department at the University of North Carolina at Greensboro for their help and support through this process.

TABLE OF CONTENTS

Page

LIST OF TABLES

Page

LIST OF FIGURES

Page

CHAPTER I

INTRODUCTION

Cardiovascular Disease: Global Impact

Cardiovascular disease (CVD) has become a significant focus of research due to the impact and devastating effects it has within the world, and in the United States. In 2017, CVD claimed more than 850,000 lives in the U.S. alone, and remains the number one cause of death [1]. Projections have shown that 45.1% of the U.S. population will have some form of CVD by the year 2035, and estimated costs are expected to jump from the $318 billion spent in 2015, to $1.1 trillion [1]. With these astronomical projections, improvements of current treatments are a crucial step in reducing these numbers. Atherosclerosis is one of the most common forms of CVD; however, it can be one of the most challenging to diagnose due to the asymptomatic nature of the disease [2]. What makes atherosclerosis even more detrimental, this disease can lead to much more complicated and life-threatening illnesses, such as myocardial infarctions, ischemic stroke and ischemic gangrene [3]. While the underlying causes of atherosclerosis are still unknown, it is understood to be triggered by an immune response of the body, leading to the formation and build-up of plaque within the arterial walls [4]. Consequently, this build-up of plaque can rupture, and is reported to be the cause of over 75% of myocardial infarctions in the U.S. [2]. With the prevalence of CVD in the U.S., and the forecasted

growth of those to be affected, understanding one of the major contributors of atherosclerosis, known as reactive oxygen species (ROS), could help scientist form a better understanding on the initiation of the disease, which could lead to a more suitable preventative

Atherosclerosis Initiation

Many risk factors have been associated with the formation of atherosclerosis, but inflammation and cellular dysfunction within the endothelial cell lining plays one of the most significant roles in the initiation process [3, 5, 6]. This endothelial cell dysfunction can be triggered by many different things; however, modified low-density lipoproteins (LDL) is one major initiator that is most commonly associated with atherosclerosis [7-9]. With the high production of ROS that is normally seen within endothelial cells, LDL can be changed into oxidized LDL once in the arterial walls [10]. This can trigger a cascading effect of positive feedback loops, allowing an increase in oxidative stress to occur and the production of more oxidized LDL [9].

As LDL pushes through the arterial walls and becomes oxidized LDL, the initiation of endothelial dysfunction/activation occurs due to the oxidative stress and ROS increase. This initiation causes the endothelial cells to signal an immune response by activating pathways that promote the expression of pro-inflammatory chemokines and cytokines such as tumor necrosis factor-alpha (TNF-α) and interleukin (IL)-8, as well as intercellular adhesion molecules (ICAM-1) [4, 7, 11, 12]. Monocytes will respond to these signals that are being released by the distressed endothelial cells and can adhere to these new expressed adhesion molecules and differentiate into macrophages. The

macrophages attempt to remove the build-up of oxidized LDL by engulfing the LDL [13]. As the macrophages take in the oxidized LDL, they will transform into foam cells, where they will begin to stick to the arterial walls and eventually undergo apoptosis [13]. When these cells undergo this programmed cell death, a release of ROS occurs, triggering another immune response from the body. [13]

Although oxidized LDL is known to be an initiator of atherosclerosis, this is not crucial in maintaining the pro-inflammatory environment [7]. TNF-α can not only be expressed highly when cells are in the presence of LDL, but also high build-ups of ROS can be a trigger for an influx of the cytokine expression [7, 14]. Alone, TNF-α can cause inflammation and even cell death through apoptosis and necrosis, and this is due to an interaction between TNF-α and the TNF receptors, such as TNFR1 [15, 16].

Current Treatments of Atherosclerosis, and the Need for Improvements

With the triggering of inflammation from oxidative stress and LDL playing a crucial role in atherosclerosis, anti-inflammatory treatments have been the direction research has been taking. Antioxidants such as Vitamin A, C, and E, have been utilized in lowering the oxidative stress and ROS production within cells [17]. These treatments; however, have not shown promising results due to the antioxidants removing not only the excess damaging ROS, but the beneficial ROS the cells need to maintain certain cellular processes [17-19].

Prescription drugs have been another method utilized in treating atherosclerosis. Statin and aspirin have been employed in attempts to lower inflammation. Statin primarily is used to lower the LDL production from the liver, in hopes to decrease the

amounts of oxidized LDL and oxidative stress. This is done by inhibiting the HMG-CoA reductase enzyme at an early stage. Aspirin is taken to lower the formation of platelets in the blood, which these platelets play a small role in producing the pro-inflammatory environment associated with atherosclerosis [20].

With using these drugs to remedy atherosclerosis and CBD, prolonged exposure can be necessary in order to see an effect of the drugs. Both long-term and short-term adverse effects have been noted when taking statin or aspirin [21]. Other remedies have been used as an attempt to reduce ROS-induced inflammation, such as using steroids and non-steroid anti-inflammatory drugs; however, these methods also incorporate a list of side-effects that can deter many individuals from using them. With this, a safe and effective method to either prevent, treat, or reverse CVD and atherosclerosis is still an ongoing search.

Nanotechnology and it's Biomedical Potential

Nanomedicine has made many advances within the biomedical community, and the treatment of many ailments using nanoparticles have been the direction many researchers have been taking. Through nanotechnology, these extremely small particles that can be less than 10 nm in size, known as carbon nanodots (CNDs), can be modified to fit the needs of the researcher, allowing to produce unique characteristics for each study [22]. These modifiable characteristics allow for expansive absorption and restricted emission ranges, along with outstanding electron donor and acceptor capabilities, and large surface area allowing for unique photoluminescent characteristics [23]. The

photoluminescent characteristics of CNDs have been the primary focus, allowing biomedical researchers to use them in bioimaging and biosensing [23-25].

Conjugating and doping CNDs with different dyes and stains are allow due to their passive surfaces, allows for the bioimaging of cancer and immune cells [23, 26]. Coupling these conjugating and doping capabilities with the extremely small size of CNDs, these dyes and stains can penetrate the cell membrane and even the nucleus with ease [23, 27]. Not only is bioimaging possible by using these photoluminescent properties, but biosensing is as well. Due to the electron donor/accepting capabilities, CNDs can quench as well as renew their luminescence, allowing for the detection of materials such as Cu2+, H2O2 and glucose [24, 28, 29]. Bioimaging and biosensing have been researched extensively, and many groups are still probing these areas; however, some have changed their direction and are looking towards using CNDs as a drug delivery method.

With CNDs biocompatibility, drug delivery is another biomedical application research has been leaning towards. Synthesis of CNDs can be extremely simple, affordable materials to make, and the materials utilized to generates these particles can modify their properties and purposes [30]. Synthesizing CNDs out of pharmaceutical drugs to treat certain ailments has been one method in researching drug delivery techniques. Aspirin-based, as well as Metronidazole-based CNDs, have been synthesized to deliver these pharmaceuticals directly to the cells, allowing for lower dosages to be effective and efficient enough [27, 31, 32]. Extensive research has been completed in this

area, along with the bioimaging and biosensing aspects of CNDs; however, the full capabilities and potential biomedical uses of CNDs have yet to be explored fully.

Carbon Nanodots Biomedical Role in Reactive Oxygen Species Scavenging

With ROS having the high affinity to bind with nearby molecules, CNDs could potentially be the vehicle needed to accept or donate molecules to these reactive oxygen compounds [33]. CNDs have been noted to be potent antioxidants and detectors of ROS, and studies have been able to demonstrate protection against these free radicals as well as oxidative stress [34]. The mechanism behind these antioxidant properties is still unclear, but the oxidant-free radical scavenging capabilities are believed to be associated with the electron donor capabilities of CNDs. The large surface area of CNDs is made up of carboxyl, hydroxyl and amino functional groups, which are believed to be responsible for the reduction and oxidation of these free radicals. Recent studies have shown that with modifications of these functional groups, antioxidant properties of CNDs increase and have extraordinary potential to facilitate future biomedical applicational purposes [35]. These antioxidant studies have demonstrated the reduction of ROS and oxidative stress in endothelial cells, yet CNDs effect can vary in different cell lines, and the interactions of many other cell types have yet to be explored. The impact of CNDs antioxidant properties on the cardiovascular system has had limited exploration. TNF-α is known to trigger the pro-inflammatory response by stimulating the production of cytokines, chemokines and adhesion molecules, causing cellular dysfunction within endothelial cells [36]. An increase in cellular ROS was reported to be involved in the inflammatory effects of TNF-α on endothelial cells [36]. However, CNDs effect on the vascular system, and

its antioxidant properties role in the anti-inflammation within vascular endothelial cells are still unclear. For this study, gene expression of pro-inflammatory cytokines, chemokines, adhesion molecules and genes associated with phase II antioxidant enzymes were examined. The potential methods of CND entry within HMEC-1s were also completed in this study, by using the fluorescent properties of these nanoparticles along with certain known channel blockers and endocytosis disruptors. This study also further tests cytotoxicity of CNDs within an *in vivo* and *in vitro* model, and found that CNDs did not possess any toxic effects or have any negative phenotypical alterations during this study.

CHAPTER II

MATERIALS AND METHODS

Cell Culture

Human Microvascular Endothelial cells (ATCC® CRL-3242™) cells will be cultured in GenDepot® MCDB131 media, supplemented with 10mM L-glutamine, 10ng/mL Endothelial Growth Factor (EGF), 1g/mL hydrocortisone, 10% Fetal Bovine Serum (FBS), and 1% Penicillin/Streptomycin. Cells were grown in Cellstar Filtered Cap 75 cm^2 cell-culture treated, filter screw cap flasks in an incubator set to 37C and 5% CO_2. Media was renewed every 2-3 days, and cells will be split into a new passage at 85-90% confluence.

CND Synthesis (JSNN)

CNDs were synthesized by collaborators in the Wei lab at the Joint School of Nanoscience and Nanotechnology. Synthesis consisted of using 0.96g citric acid, 1mL ethylenediamine and 1mL deionized water, which were mixed in glass vials and heated in a microwave reactor (300W) for 18 minutes. The temperature was maintained below 150C to result in the creation of a brown solid that was then diluted in 5mL of deionized water and dialyzed through a dialysis membrane with MWCO of 100Da for 24 hours.

CND and TNF-α Treatments

Human Microvascular Endothelial cells (HMEC-1) were treated with 10 ng/mL of TNF-α for 6 hours with a dose-dependent co-treatment of 0.03, 0.1 and 0.3mg/mL CNDs in Sigma-Aldrich/Millipore Sigma® Hanks Balanced Salt Solution (HBSS) containing calcium, magnesium, and glucose. Cells were split into 100mm x 10mm Corning® Cell Culture-treated petri-dishes and grown to 85-90% confluence. Petri dishes were decanted of their media and rinsed 2 times with 1X Phosphate Buffer Solution (PBS). 7mL of treatment were then pipetted onto adherent HMEC-1s and maintained in an incubated at 37C and 5% CO_2 during treatment.

CND Characterization

The Cary® Eclipse™ Fluorescence Spectrophotometer was used for UV-Vis spectroscopy. CNDs were diluted to a 2mg/mL concentration in deionized water and the fluorescence properties were measured in a quartz cuvette. CNDs were exposed to a wavelength of 350nm.

CND Uptake Assay

HMEC-1 cells were cultured to 85% confluency in 100mm x 10mm Corning® cell culture-treated Petri dishes. Cells were then washed 2 times with PBS and incubated for 30 minutes in HBSS and varying concentrations of known inhibitory reagents. After 30 minutes, cells were washed two times and incubated for 6 hours with 0.1mg/mL CNDs. Once 6-hour treatment was completed, treatment was removed and cells were washed 2 times with PBS to remove any excess CNDs. Cells were collected using the cell scrapping method, centrifuged at 5,000 RCF for 5 minutes and resuspended in 1mL PBS.

150μL of resuspended cells was then aliquoted into 4 wells on a black 96-well Costar® plate. The fluorescence of the plate was then read using the Bio-Tek® Synergy 2™ plate reader at 360/40 excitation and 460/40 emission.

CND Release Assay

HMEC-1 cells were grown in Costar® 6-well clear cell-culture treated plate to 85-90% confluency. Cells were washed 2 times with PBS and treated with 0.1mg/mL of CNDs in HBSS for 6 hours. Cells were then washed one time in PBS, and incubated in 300μl/well PBS for 5, 10, 15, 30 and 60 minutes. After incubation, the supernatant was collected, spun down in a centrifuge at 5,000 RCF for 5 minutes and the supernatant was then collected again and pipette into a black 96-well Costar® plate. The fluorescence of the plate was then read using the Bio-Tek® Synergy 2™ plate reader at 360/40 excitation and 460/40 emission.

CND Release Assay with Endocytosis Inhibitor

HMEC-1 cells were grown in Costar® 6-well clear cell-culture treated plate to 85-90% confluency. Cells were washed 2 times with PBS and treated with 0.1mg/mL of CNDs in HBSS for 6 hours. Cells were then washed one time in PBS, and incubated in 300μl/well PBS and with inhibitors at concentrations listed above for 30 minutes. After incubation, the supernatant was collected, spun down in a centrifuge at 5,000 RCF for 5 minutes and the supernatant was then collected again and pipette into a black 96-well Costar® plate. The fluorescence of the plate was then read using the Bio-Tek® Synergy 2™ plate reader at 360/40 excitation and 460/40 emission.

Cell Viability with Trypan Blue and Guava® ViaCount™

HMEC-1 cells were grown in 100mm x 10mm Corning® cell culture-treated Petri dishes to 85-90% confluency. Cells were then washed 2 times with PBS and treated with inhibitors for 30 minutes. After 30 minutes, treatment was removed and cells were washed with PBS 2 times. Cells were then collected using a cell scraper and spun down in a centrifuge at 5,000 RCF for 5 minutes. Cells were then resuspended in 1mL of PBS. 10µL of cell suspension was collected and 10µL of Gibco™ Trypan Blue Solution (0.4%) was added. 10µL of the cell-Trypan Blue mixture was pipetted into hemocytometer and cell viability was determined.

HMEC-1 cells were grown in either 100mm x 10mm Corning cell culture-treated Petri dish or 6- Costar® plates to 85-90% confluency. Cells were then washed two times and treated with inhibitors for 30 minutes. After the 30-minute incubation, cells were decanted and washed two times with PBS. Cells were then removed by using cell scraping, and spun down into a pellet by centrifuging them for 5 minutes at 5,000 RCF. The cells were then resuspended so that $5x10^6$ cells/1mL cold PBS were present. 80µL of resuspended cells were removed and 20µl of Millipore ViaCount™ and incubated at room temperature for 15 minutes. 500µL of cold PBS was added to the mixture after incubation. Cells were then analyzed with the Guava® EasyCyte™ Cytometer System.

Cell Viability with MTT Assay

HMEC-1 cells were grown in 24 well Costar® cell culture-treated plate to 85-90% confluency. Media was removed and cells were washed 2 times with PBS. Cells

were then treated in 150μL/well of HBSS with 0.001, 0.03, 0.1, 0.6 and 1.2mg/mL of CNDs for 6 hours. After treatment, cells were decanted and washed with 500μL/well of PBS and then replaced with 0.2g/mL MTT in 200μL HBSS and incubated for 2 hours. Following incubation, The MTT-mixture was removed and cells were washed with PBS. 200μL of dimethyl sulfoxide (DMSO) was added to each well. The plate was covered and then placed on a shaker at low speed for 15 minutes. After purple formazan crystals that had formed were dissolved, cells were then read with the Bio-Tek® Synergy 2™ plate reader at 570nm wavelength.

RNA Extraction

HMEC-1 cells were culture within the 100mm x 10mm Corning® cell culture-treated Petri dishes to 90% confluency. The media was discarded and cells were washed with 1X PBS and treated in the TNF-α/CND concentrations previously described, for 6 hours. After treatment, cells were decanted and 1mL of ambion TRIzol® was added to cells, and 1mL of mixture was pipetted into a 1.5mL Eppendorf tube. 200μL of Chloroform was added and incubated for 5 minutes at room temperature. Cells were then spun down in a centrifuge at 12,000 RCF for 15 minutes. The top aqueous layer was removed and combined with 500μL of 2-propanol, mixed well and incubated at room temperature for 15 minutes. The mixture was then centrifuged at 12,000 RCF for 10 minutes. Pellet formation occurred and washed with 1mL of 75% ethanol, centrifuged again ay 7,400 RCF for 5 minutes. Washing step was repeated once more. Pellet was then

dried and RNA was dissolved in 10μL of Nase-free diethylpyrocarbonate (DEPC) – treated water.

cDNA Synthesis

HMEC-1 cells were cultured, treated and RNA extraction was performed as listed above. The RNA extracted was quantified using Thermo Scientific NanoDrop™ and diluted to a 500ng/μL concentration. 5μL of 5X First Strand Buffer, 1.25μL of deoxynucleotide triphosphate (dNTP) solution, 1.25μL of Random Primer and 0.625μL of Moloney Murine Leukemia Virus Transcriptase (MMLV-RT) and 14.875μL of DEPC water with 2μL of diluted RNA. The 25μL solution was converted to cDNA using the Applied Biosystems ™ Veriti ™ 96-Well Thermal Cycler.

Quantitative Real Time-Polymerase Chain Reaction (qRT-PCR)

Cells were treated, RNA extracted, and cDNA synthesized as previously described. The cDNA will be used to target genes of interest by combining 10μL of Power SYBR® Green PCR Master Mix, 5μL of DEPC water, 2μL of forward primer and 2μL of reverse primer for the genes of interest with 1μL of the diluted (1:9) cDNA. The genes of interest will be IL-8, ICAM, MCP-1, IL-1β, GCLC and HO-1 with GAPDH serving as the housekeeping gene. The Applied Biosystem® StepOnePlus™ Real-Time PCR system ran for 40 cycles. Each cycle will be as followed: 95C for 15 seconds, 58C phase for 1 minute and a 60C cycle for 10 seconds. To quantify gene expression, the comparative threshold cycle (C_T) values were used.

IDT® Human Primer Sequences

The primer sequences are listed as followed: GAPDH Forward: 5' AGA ACG GGA AGC TTG TCA TC – 3', GAPDH Reverse: 5' – GGA GGC ATT GCT GAT GAT CT – 3'. IL-8 Forward: 5' CTC TGT GTG AAG GTG CAG TT – 3', Reverse: 5' AAA CTT CTC CAC AAC CCT CTG – 3'. ICAM Forward: 5' ACA GTG ACC ATC TAC AGC TTT C – 3', Reverse: 5'- CGG GTC TGG TTC TTG TGT ATA A – 3'. MCP-1 Forward: 5'- GCT CAG CCA GAT GCA ATC AA – 3', Reverse: 5'- GGT TGT GGA GTG AGT GGT CAA G – 3'. IL-1β Forward: 5'-CCA GCT ATG AAC TCC TTC TC-3', Reverse: 5'-GCT TGT TCC TCA CAT CTC TC-3'. NQO-1 Forward: 5' – TTA CTA TGG GAT GGG GTC CA – 3', NQO-1 Reverse: 5' – TCT CCC ATT TTT CAG GCA AC – 3'. GCLC Forward: 5' – ACC ATC ATC AAT GGG AAG GA – 3', GCLC Reverse: 5' – GCG ATA AAC TCC CTC ATC CA – 3'. AR Forward: 5' - TGG ATG GAT AGC TAC TCC GG - 3', Reverse: 5' - CCC AGA AGC TTC ATC TCC AC - 3'.

Animal Project (Protocol 20-003)

Male C57BL/6 mice were purchased from Jackson Laboratory at 10 weeks of age. Mice were initially weighed and placed into three groups: 9 mice in the control, 9 mice in the TNF-α group, and 12 mice in the TNF-α + CND. Treatment began and intraperitoneal injections were given daily. Mice in the control group received 100μg of sterile saline, the TNF-α group was dosed based off body weight (25μg/kg), and the TNF-α + CND group received dosages based off body weight (25μg/kg TNF-α + 2.5mg/kg CNDs). Mice had bedding changed twice a week, on Tuesday and on Friday, and their food and water checked daily. Once treatment was complete, mice were

sacrificed using isoflurane and confirmation of sedation performed by checking for the absence of withdrawal reflex of hindlimb by toe pinch. Blood was collected by cardiac puncture and tissues harvested for further, future studies.

CHAPTER III

RESULTS

Characterization of CNDs: UV-Vis

The Cary® Eclipse™ Fluorescence Spectrophotometer was used for characterizing the CNDs. The photoluminescent characteristics of CNDs can be seen in their excitation wavelength around 360nm and expressed an emission peak around 460nm (Fig. 1). Understanding the excitation and emission spectra CNDs fall within allows for utilizing this information for the detection of the nanoparticles during uptake assays.

Cell Viability with MTT

Before looking into potential anti-inflammatory properties of CNDs, it is important to determine if CNDs display any toxic effects to endothelial cells. A colorimetric assay known as an MTT assay was completed to analyze the mitochondrial function of HMEC-1 cells treated with 0.001, 0.03, 0.1, 0.3, 0.6, and 1.2 mg/mL of CNDs for 6 hours (Fig. 2). MTT is a positively charged tetrazolium compound that can easily penetrate viable eukaryotic cells [37]. A viable cell is able to convert the MTT with their mitochondria, into an insoluble, purple product known as formazan. DMSO is then used to dissolve the formazan, making the color much more stable and readable at 570nm wavelengths [37]. CNDs at all tested concentrations did not demonstrate any significant

($P > 0.05$) toxic effects when compared to the control, suggesting there is no significant change in mitochondrial function with CND treatments.

Quantitative Real Time-Polymerase Chain Reaction (qRT-PCR) for Proinflammatory Genes

We next wanted to determine the effect of CND's on proinflammatory biomarkers in endothelial cells. HMEC-1 cells were treated with 0.03, 0.1 or 0.3 mg/mL of CND in the presence of 10ng/mL of TNF-α for 6 hours. After the 6-hour treatment, cells underwent RNA extraction, cDNA synthesis and qRT-PCR analysis.

Our studies show IL-8 gene expression significantly decreased ($P < 0.05$), with cells that were co-treated with TNF-α and either 0.03, 0.1 and 0.3 mg/mL of CNDs, when compared to the cells treated with only TNF-α (Fig. 3A). ICAM is another gene that is associated with proinflammatory cellular distress in endothelial cells. During our studies, when looking at ICAM gene expression during our treatment, the co-treatment of TNF-α with 0.3 mg/mL of CNDs displayed a significant decrease ($P < 0.05$), in gene expression when compared to cells treated with TNF-α alone (Fig. 3B). We also found that cells treated with a co-treatment of TNF-α and either 0.1 or 0.3 mg/mL of CNDs had a significant decrease ($P < 0.05$), in gene expression of IL-1β, when compared to cells only treated with TNF-α (Fig. 3C). Pro-inflammatory chemokine MCP-1 was also analyzed due to its important role in attracting monocytes to endothelial cells undergoing stress [38]. When analyzing MCP-1 with the qRT-PCR data, we found no significant difference in gene expression of any co-treated HMEC-1 cells ($P > 0.05$), when compared to cells treated with on TNF-α (Fig. 3D).

Quantitative Real Time-Polymerase Chain Reaction (qRT-PCR) for ROS Detoxification Gene Expression

Antioxidants are known for their role in mediating inflammation, while ROS is known to be an inductor. We wanted to see if the anti-inflammatory effects of CNDs are associated with their potential changes in expression of ROS detoxification genes such as NAD(P)H: Quinone Oxidoreductase 1 (NQO1), Nuclear factor erythroid 2 (Nrf2), aldose reductase (AR), Glutathione reductase (GR), Glutamate-Cysteine Ligase Catalytic Subunit (GCLC) and Heme Oxygenase 1 (HO-1). Treatment for HMEC-1 cells were followed as previously described, with a co-treatment of TNF-α and either 0.03, 0.1 or 0.3 mg/mL of CNDs for 6 hours. After treatment, RNA extraction, cDNA synthesis, and qRT-PCR were completed.

HO-1 is an important antioxidant that has the ability to protect endothelial cells from apoptosis. Previous studies have found that the overexpression of HO-1 can reduce TNF-α induced expression of proinflammatory genes such as E-selectin, ICAM and Vascular adhesion molecule (VCAM), along with reducing the activation of the transcription factor, Nuclear Factor κ-light-chain enhancer (NF-κB) [39]. During our analysis, a significant increase in gene expression ($P < 0.05$), was seen for cells treated with a co-treatment of TNF-α and 0.3mg/mL when compared to cells treated with only TNF-α (Fig. 4A). NQO1 is another important antioxidant that is a quinone reductase, responsible for protecting cells from producing excess levels of ROS [40]. Our studies have shown that CNDs have no effect on NQO1 gene expression ($P > 0.05$), when comparing the co-treated TNF-α and CND cells with cells treated only with TNF-α (Fig.

4B). Nrf2 is a transcription factor that can activate expression of promoters apart of the antioxidant response element (ARE), which are responsible for maintaining levels of ROS. Activation of Nrf2 has shown to be a potential method in reducing CVD [41]; however, our results demonstrate that CNDs have no significant effect on Nrf2 gene expression ($P > 0.05$), with co-treated cells compared to only TNF-α treated cells (Fig. 4C). We wanted to see if CNDs had any effect on gene expression of another ROS modulator known as AR. Our results demonstrate that the co-treatment with TNF-α and CNDs had no significant change in gene expression ($P > 0.05$), of AR in HMEC-1s (Fig. 4D). GR is another important antioxidant enzyme that catalyzes the reduction of glutathione disulfide (GSSG) to the sulfhydryl form glutathione (GSH) [42]. Previous studies have shown that GR knockout mice had an increase in proinflammatory cytokines such as TNF-α and IL-6 [43]. Results demonstrated no change ($P > 0.05$), in gene expression of GR comparing our co-treated HMEC-1s with cells treated only with TNF-α (Fig. 4E).

CND Uptake Assay

Determining the possible routes of entry of CNDs is important to understand the function and role these nanoparticles have in the cell. Uptake had previously been studied in our lab using HMEC-1 cells, where cells were treated with 0, 0.03, 0.1, 0.2 and 0.3 mg/mL CNDs for either 6 or 12 hours. Results displayed a dose-dependent increase in fluorescence for both the 6- and 12-hour treatments [44]. For determining possible route of entry within HMEC-1 cells, different inhibitors were tested individually to determine if any of them had the capability to reduce CND fluorescence. Endocytosis has been

suggested to be the route of uptake for CNDs from previous research completed with different cell lines and different sized nanoparticles [45]. HMEC-1s were treated with endocytosis disrupting inhibitors for 30 minutes with concentrations determined from previous studies (Table 1). Inhibitors were removed, cells were washed two times with 1X PBS and treated with 0.1 mg/mL of CNDs. Cells were then washed two times with 1X PBS to ensure any excess CNDs were removed. Using HMEC-1 cells showed a significant decrease ($P < 0.05$) in fluorescent intensity when cells were pre-treated with phenylglyoxal, which is a known selective phagocytic inhibitor (Fig. 6A). Chlorpromazine HCL (Fig. 6B), which is known to suppress clathrin disassembly, also had a significant change in fluorescence, showing a potential increase in CND uptake ($P < 0.05$). Other endocytosis disrupting inhibitors were tested (Fig. 8A-C) and demonstrated no significant change in fluorescence of CNDs ($P > 0.05$).

Channel blocking inhibitors were also tested due to CND's known ability for having a slight negative charge [46, 47]. HMEC-1s were this time treated for 30 minutes with known channel blocking inhibitors at concentrations from previously completed research (Table 1). After the 30-minute treatment, the 6-hour CND treatment with 0.1mg/mL began, and once treatment was completed, cells were washed two times with 1X PBS to ensure the removal of excess CNDs. Amlodipine (Fig. 6C), a known calcium channel blocker, showed a significant increase in fluorescence intensity ($P < 0.05$). Further studies were completed using other channel blockers (Fig. 7A-L), which all showed no significant changes in fluorescent intensity ($P > 0.05$).

CND Release Assay

After determination of the potential route of uptake, understanding the rate at which CNDs were released from HMEC-1s. To do this, HMEC-1s were treated with 0.1 mg/mL of CNDs for 6 hours. After the 6-hour treatment, cells were gently washed two times with 1X PBS. Cells were then incubated with 300µl of PBS, and the supernatant was collected at 0, 5, 10, 15, 30 or 60 minutes after adding PBS (Fig. 9). The supernatant was spun down and the supernatant was collected again, to ensure if any cells that had died were collected, their fluorescence would not be read. At 15, 30 and 60 minutes, a significant increase in fluorescence of CNDs was detected ($P < 0.05$).

CNDs Release with Endocytosis Inhibitors

After determining the times for release and the inhibitors that potentially affect the uptake of CNDs, release using these inhibitors was completed to determine if any effect occurred on the expulsion of the CNDs. HMEC-1 cells were treated for 6 hours with 0.1 mg/mL of CNDs. After treatment, cells were washed two times and incubated with either phenylglyoxal (Fig. 10A), or chlorpromazine HCL (Fig. 10B) with their previously described concentrations (Table 1), for 30 minutes. Phenylglyoxal showed no significant change in fluorescent intensity ($P > 0.05$), while Chlorpromazine HCL showed a significant increase in CND fluorescent intensity during the 30-minute release ($P < 0.05$).

Cell Viability with Trypan Blue and Guava® ViaCount™

Since phenylglyoxal (Fig. 7A), displayed a significant decrease in uptake ($P < 0.05$), making sure that the decrease was not due to a decrease in viability needed to be

determined. HMEC-1 cells were treated with phenylglyoxal at the concentration previously described (Table 1), for 30 minutes. The cells were then washed two times with 1X PBS and incubated in HBSS for 6 hours. After incubation, cells were washed two times and removed for cell viability check using trypan blue (Fig, 12A). Trypan blue is dye that is unable to permeate through cells unless the membrane has been compromised. If the dye is capable of entering the cell, it will bind to proteins found within the HMEC-1s, making it blue in color. Our results displayed no significant change in cell viability from the use of phenylglyoxal ($P < 0.05$).

ViaCount™ was then completed to further demonstrate cell viability of HMEC-1 cells with phenylglyoxal. HMEC-1 cells were treated with previously described concentrations of phenylglyoxal (Table 1), for 30 minutes. After the incubation, cells were washed two times, removed, and the ViaCount™ was completed (Fig. 12B-D). ViaCount™ reagent contains two different dyes that binds to DNA, and has the ability to give both a cell count and cell viability reading. One dye is able to bind to DNA in all cells, allowing them to get the count of cells present regardless if cells are dead or alive. The second dye binds to the DNA of cells that are dead, allowing for a viability count. Depending on the strength of the binding for the viability dye allows for the assay to distinguish apoptotic cells. Our results demonstrated no significant change in cell viability when treated with the endocytosis disrupting inhibitor ($P > 0.05$).

Animal Project (Protocol 20-003)

C57BL/6 male mice at 10 weeks of age were placed into three different groups and were administered with either 100μg of sterile saline, 25μg/kg of TNF-α, or 25μg/kg

TNF-α + 2.5mg/kg CNDs for one week. The dosing occurred daily, and mice were weighed each day to ensure correct dosing. During the exposure, the body weight was collected (Fig. 13), and showed no significant change ($P > 0.05$) when comparing to the group given the control substance of 100μL of saline. This demonstrates that CNDs have no phenological effect.

CHAPTER IV

DISCUSSION

TNF-α is a known proinflammatory cytokine and can trigger a positive feedback loop, producing more TNF-α along with other proinflammatory cytokines, chemokines and adhesion molecules [7]. This study demonstrated that CNDs have the potential to reduce TNF-α induced inflammation in HMEC-1s by reducing the release of proinflammatory cytokines and chemokines. IL-8's relative gene expression was significantly reduced with the co-treatment of CNDs, which could read to a reduction of monocyte response. Studies completed in our lab have previously looked at any changes in HMEC-1's phase II antioxidant enzyme activity as well as gene expression for these enzymes when treated with CNDs, and results found that there were no changes in either [44]. However, no studies have been completed to see the effects of gene expression of phase II antioxidant enzymes during a co-treatment with TNF-α and CNDs. In our study, HO-1 relative gene expression saw a significant increase, demonstrating that CNDs are not only free radical scavengers, but could potentially affect gene expression in genes related to phase II enzymes. Our studies also explored CND uptake release routes by using the fluorescent characteristics of these nanoparticles. Two endocytosis disruptors and one channel blocking inhibitor displayed significant changes in CND uptake when compared to cells treated with only CNDs. Further analysis of the effect these

endocytosis disruptors had on the release of CNDs was tested, and showed that chlorpromazine HCL significantly increase CND fluorescence, suggesting an increase in CND release. Furthermore, exploration of the cytotoxicity of CNDs was tested, and these nanoparticles did not appear to display toxic effects during both *in vivo* and *in vitro* trials. Through MTT and C57BL/6 mice exposure, it was demonstrated that CNDs display little to no cytotoxic effects. Collectively, these finding suggests a potential anti-inflammatory action of CNDs against endothelial inflammation.

Monocyte adhesion to endothelial cells is the initial stage for the formation of atherosclerosis. Inflamed endothelial cells release a storm of cytokines, chemokines and increase expression of their adhesion molecules, triggering a fast response of the immune system [4, 11, 48]. Immune cells, such as monocytes, respond by adhering to the distressed endothelial cell, and the process of transendothelial migration occurs [49]. During this event, signals between the endothelial cell and monocyte are relayed, eventually leading to the differentiation and migration of the monocyte between the endothelial cells and traveling to the site of inflammation [49]. The activated macrophages begin to engulf the stress-inducing materials such as oxidized LDL. The engulfing of oxidized LDL causes the macrophages to transform into foam cells, which stick to and build up in the arterial walls, undergo apoptosis, and causes the formation of atherosclerosis plaque [13]. Atherosclerosis is typically associated with larger blood vessels found within the cardiovascular system, such as the aorta, due to the appearance of the disease first occurring in these areas; however, smaller blood vessels have been affected with atherosclerotic lesions usually later with age, and for this reason, HMEC-1s

were selected for this study [50]. This endothelial cell line that has been immortalized is commonly used for investigation of CVD due to their ability to retain many endothelial characteristics, such as the expression of ICAM and their ability to uptake LDL, and they have also been widely characterized [51].

IL-8 is a proinflammatory cytokine, that can cause an extremely rapid response from the immune system, and it has been shown to be highly expressed during cellular dysfunction of endothelial cells [52, 53]. It has been shown in previous studies that when endothelial cells were treated with TNF-α, a dose-dependent increase in IL-8 gene expression was noticed [54]. ICAM is an adhesion molecule and is typically always present on the cell membrane of endothelial cells; however, during cellular stress, an influx in gene expression and appearance of the adhesion molecule are indicators of dysfunction [55, 56]. The increase of this adhesion molecule is essential during the initiating process of atherosclerosis. Because of this molecule, monocytes and other leukocytes are able to bind to these distressed endothelial cells, and the transmigrational event occurs [57]. IL-1β is another proinflammatory cytokine, that is responsible for increased vascular permeability of endothelial cells, while MCP-1 is a chemoattractant that is responsible for recruiting monocytes to the inflamed area [38, 58]. The activation of these proinflammatory molecules is a biomarker for endothelial cell dysfunction and inflammation [38, 52, 54-56, 58]. Our study, for the first time, has shown that CND treatment significantly suppressed TNF-α induced expression of IL-8, ICAM and IL-1β, suggesting a potential anti-inflammatory action of CNDs against vascular dysfunction.

Our study was unable to determine the mechanism by which CNDs reduces TNF-α induced inflammation, and is an area that requires further exploration. However, the ability of ROS scavenging by CNDs could be the mechanism that contributes to the pro-inflammatory properties based on two of the following reasons. First, researchers have demonstrated that CNDs have the capability to be free radical scavengers through DPPH• testing. DPPH• is a fluorescent test, where transferring of an electron either through oxidation or reduction, can stabilize, and reduce the fluorescent reading. It was demonstrated that CNDs reduced the fluorescence of DPPH, demonstrating antioxidant, free radical scavenging potentials [33]. Within our lab, it was demonstrated through EPR, that CNDs are ROS scavengers for hydroxyl and superoxide anions with concentrations as low as 0.01mg/mL [44] Secondly, excess ROS and its subsequent oxidative stress are known to induce vascular inflammation [59, 60]. An increase in cellular ROS was reported to be involved in the inflammatory effects of TNF-α on endothelial cells [36]. While ROS can occur naturally, and the bulk of it for endothelial cells can come from the mitochondrial leakage, it has been reported that NADPH oxidase activation occurs with TNF-α [61, 62]. NADPH oxidase is an enzyme responsible for facilitating the production of superoxide anions by removing an electron from NADPH, and passing it to oxygen. This transfer of electrons case a redox cycle to form and overproduction of ROS [63]. These literatures provided by this previous research supports the possibility that CNDs have ROS scavenging activity, and may be the explanation for the anti-inflammatory effects these nanoparticles have on lowering the TNF-α induced proinflammatory biomarkers in our study.

ROS can also be regulated by NQO1, Nrf2, GCLC, GR, AR, and HO-1 [39-41, 43, 64]. Our study investigated if this anti-inflammatory effect CNDs can be explained through changes in ROS modulator molecules in endothelial cells. However, our results showed no change in gene expression for the gene associated with the ROS modulator molecules except for HO-1. Interestingly, HO-1 gene expression had a significant increase with cells co-treated with CNDs at 0.3mg/mL and TNF-α, and an increase like this due to CNDs has never been reported before. HO-1 has antioxidant, anti-inflammatory characteristics through cytoprotective qualities, and is able to reduce apoptosis and reduce cellular distress [65, 66]. Previous studies have shown higher susceptibility to oxidized LDL injury and H_2O_2-induced apoptosis in HO-1 knockout mice [67]. HO-1 is an enzyme that, when in the presence of three oxygen molecules, NADPH and cytochrome p450, is able to catalyze heme into biliverdin, ferrous iron and carbon monoxide [68]. Biliverdin can be further broken down by biliverdin reductase and NADPH into bilirubin, an important biomolecule that helps removed abnormal and aged red blood cells [68]. This removal of toxic heme can also be beneficial for healthy vascular function, and protection of the endothelial lining [69]. Studies have shown that HO-1 gene expression at basal levels is typically low, but with an increase in those basal levels, endothelial cells expressed lower basal levels of proinflammatory cytokine IL-1β and adhesion molecule ICAM [65, 70]. This is consistent with our findings of a decrease in gene expression of IL-1β and ICAM, and an increase in HO-1 expression when HMEC-1s were co-treated with TNF-α and 0.3mg/mL of CNDs. This reasoning behind the spike in HO-1 gene expression by CNDs is still unclear, but the Nrf2 pathway could

explain the change [39, 71]. Nrf2 is a transcription factor that is found in the cytosol of a cell, and is sequestered by keap1. During cellular stress, ubiquitination occurs, allowing for the removal of keap1, and the transnuclear location of the Nrf2 transcription factor to enter and promote gene expression of antioxidants such as HO-1 [72]. Future studies will be needed to examine if the activation of the Nrf2 pathway occurs in HMEC-1s by CNDs, which could further explain the decrease in proinflammatory genes.

As an Nrf2-mediated gene, HO-1 also plays a vital role for Nrf2-mediated NF-κB inhibition by playing an important mediator for the cross-talk between Nrf2 and NF-κB response pathways. [39, 71]. NK-κB is a transcription factor made up of RelA and P65, and found in the cytoplasm, bound to the inhibitor, IκBα. This pathway can be activated through the presence of cellular distress such as TNF-α or ROS, and triggers a phosphorylation and ubiquitination of the bound IκBα, freeing this transcription factor and allowing it to translocate into the nucleus and bind to the designated promotor region, triggering an increase in gene expression of proinflammatory cytokines [7, 73]. The upregulation of HO-1 via the Nrf2 pathway was found to limit the production of proinflammatory cytokines from the NF-κB pathway [39, 71, 73]. Future studies are necessary to determine if the increased gene expression of HO-1 results in an increase in enzyme production of heme oxygenase. Also, the effect HO-1 has on the NK-κB pathway could be tested by using the eLucidate™ RAW 264 NF-κB Reporter Cell Line This is a macrophage cell line derived from mice, and contains Renilla luciferase, integrated into, and can be activated as a response with the NF-κB activation [74]. An

NF-κB nuclear translocation assay could also be completed by using a dyed antibody that will attach to the p65 portion of the NF-κB transcription factor. A confocal microscope can determine the location of the p65: if the dye is inside the nucleus, then activation of the pathway occurred, if it remains in the cytoplasm, it was not activated. The examination of the NF-κB pathway is important to help further explain the possible reasoning that our 0.3mg/mL of CNDs showed a decrease in proinflammatory cytokines, and an increase in the high HO-1 gene expression when HMEC-1s experience TNF-α induced inflammation.

To further understand the action CNDs have on HMEC-1 cells, we studied the uptake and release of these nanoparticles. Diffusion, protein channels or through endocytosis were the routes believed these nanoparticles could take; however, diffusion has been quickly ruled out due to the negative charge CNDs have [75]. Previous studies have been completed using different types of nanoparticles and different cell lines to examine potential routes of uptake. One study utilized HeLa, a cervical cancer cell line, and glycol chitosan nanoparticles. Different reagents were employed as potential inhibitors, to examine if they have any effect on the uptake of these nanoparticles. Chlorpromazine HCL was used due to the ability to inhibit clathrin-mediated endocytosis. Amiloride was used to inhibit micropinocytosis [76]. Results showed that these nanoparticles followed no particular route of endocytosis [76]. Another study used carboxylated polystyrene nanoparticles at either 40 nm or 200 nm in size in HeLa, A549 (lung carcinoma), and 1321N1 (brain astrocytoma) cell lines. Chlorpromazine HCL was used again along with genistein, which is an inhibitor of tyrosine kinase, cytochalasin A,

an actin disruptor, and nocodazole, another chlathrin-mediated endocytosis [45]. Results from this study showed that particle size and cell type all played a part to the method of uptake [45]. In our study, we are exploring the effect of these inhibitors, along with other reagents that are known as endocytosis disruptors. Our results showed that phenylglyoxal, a known phagocytosis inhibitor [77], significantly reduced the fluorescence of CNDs. Chlorpromazine HCL, a clathrin disruptor, also reduced the fluorescence significantly. We began exploring other inhibitors, such as channel blockers, to see if other routes of uptake are possible due to the characteristics CNDs have [75]. After exploring our selected known channel blocking inhibitors, the results displayed that amlodipine, a calcium channel blocker [78], increased the fluorescence of CNDs. Previous studies completed on human umbilical vein endothelial cells (HUVEC) suggested that when a build-up of calcium occurs internally within endothelial cells, this stimulates an increase in endocytosis events [79]. If amlodipine inhibits not only the uptake, but also the release of calcium, this could be an explanation for the increase in CND uptake our results showed. Our results showed that phenylglyoxal and chlorpromazine significantly decreased CND uptake, while amlodipine increased it, supporting that CNDs route of uptake might not only be through endocytosis. Limitations can be noted about this assay, due to the lack of a positive control, determining if the known inhibitors effects are working is unknown. Because this assay utilizes fluorescence, and each known inhibitor effects different uptake mechanisms, it would be challenging to determine positive controls fit for this experiment. This study suggests possible methods; however, further testing is required. Release of the CNDs were to be

explored next, and we began by looking at the how the inhibitors effecting uptake, might potentially affect release. Phenylglyoxal had no significant change in fluorescence, while chlorpromazine significantly increased fluorescence during release. With chlorpromazine effecting uptake with a decrease, and effecting release with an increase, this further suggests and supports the idea that CNDs route of uptake and release are not always the same, and different pathways could be used for release of these nanoparticles.

In summary, HMEC-1 endothelial inflammation that was induced by 10ng/mL of TNF-α can be mediated with CNDs at concentrations ranging from 0.1-0.3mg/mL. TNF-α was able to stimulate a change in proinflammatory biomarkers in HMEC-1s, and CNDs were found to counteract them. Our results showed CNDs did not possess cytotoxic characteristics when cells were treated with concentrations as high as 1.2mg/mL for 6 hours. Furthermore, our study was able to narrow down potential routes of uptake for CNDs into HMEC-1s, showing that endocytosis is indeed a route of entry; however, it might not be the only. These findings provide insights on the interaction CNDs and endothelial cells undergoing TNF-α induced cellular inflammation.

REFERENCES

1. Virani, S.S., et al., *Heart Disease and Stroke Statistics-2020 Update: A Report From the American Heart Association.* Circulation, 2020. **141**(9): p. e139-e596.
2. Pahwa, R. and I. Jialal, *Atherosclerosis*, in *StatPearls*. 2020: Treasure Island (FL).
3. Hansson, G.K., *Inflammation and Atherosclerosis: The End of a Controversy.* Circulation, 2017. **136**(20): p. 1875-1877.
4. Moss, J.W. and D.P. Ramji, *Cytokines: roles in atherosclerosis disease progression and potential therapeutic targets.* Future Med Chem, 2016. **8**(11): p. 1317-30.
5. Davignon, J. and P. Ganz, *Role of endothelial dysfunction in atherosclerosis.* Circulation, 2004. **109**(23 Suppl 1): p. III27-32.
6. Libby, P., *Inflammation in atherosclerosis.* Arterioscler Thromb Vasc Biol, 2012. **32**(9): p. 2045-51.
7. Tedgui, A. and Z. Mallat, *Cytokines in atherosclerosis: pathogenic and regulatory pathways.* Physiol Rev, 2006. **86**(2): p. 515-81.
8. Ramji, D.P. and T.S. Davies, *Cytokines in atherosclerosis: Key players in all stages of disease and promising therapeutic targets.* Cytokine Growth Factor Rev, 2015. **26**(6): p. 673-85.
9. Yoshida, H. and R. Kisugi, *Mechanisms of LDL oxidation.* Clin Chim Acta, 2010. **411**(23-24): p. 1875-82.
10. Turrens, J.F., *Mitochondrial formation of reactive oxygen species.* J Physiol, 2003. **552**(Pt 2): p. 335-44.
11. Mehra, V.C., V.S. Ramgolam, and J.R. Bender, *Cytokines and cardiovascular disease.* J Leukoc Biol, 2005. **78**(4): p. 805-18.
12. Nallasamy, P., et al., *Sulforaphane reduces vascular inflammation in mice and prevents TNF-α-induced monocyte adhesion to primary endothelial cells through interfering with the NF-κB pathway.* The Journal of nutritional biochemistry, 2014. **25**(8): p. 824-33.
13. Samson, S., L. Mundkur, and V.V. Kakkar, *Immune response to lipoproteins in atherosclerosis.* Cholesterol, 2012. **2012**: p. 571846.
14. Varfolomeev, E. and D. Vucic, *Intracellular regulation of TNF activity in health and disease.* Cytokine, 2018. **101**: p. 26-32.
15. Marks, F., U. Klingmüller, and K. Müller-Decker, *Cellular signal processing : an introduction to the molecular mechanisms of signal transduction*. Second edition. ed. 2017, New York, NY: Garland Science.

16. Hsu, H., et al., *TRADD-TRAF2 and TRADD-FADD interactions define two distinct TNF receptor 1 signal transduction pathways.* Cell, 1996. **84**(2): p. 299-308.
17. Panth, N., K.R. Paudel, and K. Parajuli, *Reactive Oxygen Species: A Key Hallmark of Cardiovascular Disease.* Adv Med, 2016. **2016**: p. 9152732.
18. Montezano, A.C. and R.M. Touyz, *Reactive oxygen species and the cardiovascular system*. 2012, Morgan & Claypool: San Rafael, Calif. (1537 Fourth Street, San Rafael, CA 94901 USA).
19. Sugamura, K. and J.F. Keaney, Jr., *Reactive oxygen species in cardiovascular disease.* Free Radic Biol Med, 2011. **51**(5): p. 978-92.
20. Hennekens, C.H. and W.R. Schneider, *The need for wider and appropriate utilization of aspirin and statins in the treatment and prevention of cardiovascular disease.* Expert Rev Cardiovasc Ther, 2008. **6**(1): p. 95-107.
21. Golomb, B.A. and M.A. Evans, *Statin adverse effects : a review of the literature and evidence for a mitochondrial mechanism.* Am J Cardiovasc Drugs, 2008. **8**(6): p. 373-418.
22. Hill, S. and M.C. Galan, *Fluorescent carbon dots from mono- and polysaccharides: synthesis, properties and applications.* Beilstein J Org Chem, 2017. **13**: p. 675-693.
23. Hoshino, A., et al., *Use of fluorescent quantum dot bioconjugates for cellular imaging of immune cells, cell organelle labeling, and nanomedicine: surface modification regulates biological function, including cytotoxicity.* Journal of Artificial Organs, 2007. **10**(3): p. 149-57.
24. Lin, L., et al., *Intrinsic peroxidase-like catalytic activity of nitrogen-doped graphene quantum dots and their application in the colorimetric detection of H2O2 and glucose.* Analytica chimica acta, 2015. **869**: p. 89-95.
25. Miao, P., et al., *Recent advances in carbon nanodots: synthesis, properties and biomedical applications.* Nanoscale, 2015. **7**(5): p. 1586-95.
26. Lee, C.H., et al., *Bioimaging of targeting cancers using aptamer-conjugated carbon nanodots.* Chemical communications (Cambridge, England), 2013. **49**(58): p. 6543-5.
27. Xu, X., et al., *Aspirin-Based Carbon Dots, a Good Biocompatibility of Material Applied for Bioimaging and Anti-Inflammation.* ACS Appl Mater Interfaces, 2016. **8**(48): p. 32706-32716.
28. Zong, J., et al., *Carbon dots as fluorescent probes for "off-on" detection of Cu2+ and L-cysteine in aqueous solution.* Biosens Bioelectron, 2014. **51**: p. 330-5.
29. Ma, J.-L., et al., *Simple and Cost-Effective Glucose Detection Based on Carbon Nanodots Supported on Silver Nanoparticles.* Analytical Chemistry, 2017. **89**(2): p. 1323.
30. Chan, K.K., S.H.K. Yap, and K.T. Yong, *Biogreen Synthesis of Carbon Dots for Biotechnology and Nanomedicine Applications.* Nanomicro Lett, 2018. **10**(4): p. 72.
31. Sun, H., et al., *Graphene quantum dots-band-aids used for wound disinfection.* ACS Nano, 2014. **8**(6): p. 6202-10.

32. Liu, J., et al., *One-step hydrothermal synthesis of photoluminescent carbon nanodots with selective antibacterial activity against Porphyromonas gingivalis.* Nanoscale, 2017. **9**(21): p. 7135-7142.
33. Zhang, W., et al., *Antioxidant Capacity of Nitrogen and Sulfur Codoped Carbon Nanodots.* ACS Applied Nano Materials, 2018. **1**(6): p. 2699-2708.
34. Das, B., et al., *Carbon nanodots from date molasses: new nanolights for the in vitro scavenging of reactive oxygen species.* J. Mater. Chem. B, 2014. **2**(39): p. 6839-6847.
35. Ji, Z., et al., *Tuning the Functional Groups on Carbon Nanodots and Antioxidant Studies.* Molecules (Basel, Switzerland), 2019. **24**(1).
36. Picchi, A., et al., *Tumor necrosis factor-alpha induces endothelial dysfunction in the prediabetic metabolic syndrome.* Circ Res, 2006. **99**(1): p. 69-77.
37. Riss, T.L., et al., *Cell Viability Assays*, in *Assay Guidance Manual*, G.S. Sittampalam, et al., Editors. 2004: Bethesda (MD).
38. Maus, U., et al., *Role of endothelial MCP-1 in monocyte adhesion to inflamed human endothelium under physiological flow.* Am J Physiol Heart Circ Physiol, 2002. **283**(6): p. H2584-91.
39. Soares, M.P., et al., *Heme oxygenase-1 modulates the expression of adhesion molecules associated with endothelial cell activation.* J Immunol, 2004. **172**(6): p. 3553-63.
40. Ross, D. and D. Siegel, *Functions of NQO1 in Cellular Protection and CoQ10 Metabolism and its Potential Role as a Redox Sensitive Molecular Switch.* Front Physiol, 2017. **8**: p. 595.
41. Satta, S., et al., *The Role of Nrf2 in Cardiovascular Function and Disease.* Oxid Med Cell Longev, 2017. **2017**: p. 9237263.
42. Couto, N., J. Wood, and J. Barber, *The role of glutathione reductase and related enzymes on cellular redox homoeostasis network.* Free Radic Biol Med, 2016. **95**: p. 27-42.
43. Goodwin, J.E., et al., *Endothelial glucocorticoid receptor is required for protection against sepsis.* Proc Natl Acad Sci U S A, 2013. **110**(1): p. 306-11.
44. Khan, S., N.C.D.O.C.o. Knowledge, and Scholarship, *Carbon nanodots in endothelial cells and C57BL/6 mice: a study of toxicity and anti-inflammatory effect*. 2018, [University of North Carolina at Greensboro]: [Greensboro, N.C.].
45. dos Santos, T., et al. *Effects of Transport Inhibitors on the Cellular Uptake of Carboxylated Polystyrene Nanoparticles in Different Cell Lines*. PLoS ONE, 2011. **6**, DOI: 10.1371/journal.pone.0024438.
46. Strauss, V., et al., *Carbon nanodots: toward a comprehensive understanding of their photoluminescence.* J Am Chem Soc, 2014. **136**(49): p. 17308-16.
47. Essner, J.B., et al., *A switchable peroxidase mimic derived from the reversible co-assembly of cytochrome c and carbon dots.* J Mater Chem B, 2016. **4**(12): p. 2163-2170.
48. Tedgui, A. and C. Bernard, *Cytokines, immuno-inflammatory response and atherosclerosis.* Eur Cytokine Netw, 1994. **5**(3): p. 263-70.

49. Muller, W.A., *Transendothelial migration: unifying principles from the endothelial perspective.* Immunol Rev, 2016. **273**(1): p. 61-75.
50. Aboyans, V., P. Lacroix, and M.H. Criqui, *Large and small vessels atherosclerosis: similarities and differences.* Prog Cardiovasc Dis, 2007. **50**(2): p. 112-25.
51. Ades, E.W., et al., *HMEC-1: establishment of an immortalized human microvascular endothelial cell line.* J Invest Dermatol, 1992. **99**(6): p. 683-90.
52. Oude Nijhuis, C.S., et al., *Endothelial cells are main producers of interleukin 8 through Toll-like receptor 2 and 4 signaling during bacterial infection in leukopenic cancer patients.* Clin Diagn Lab Immunol, 2003. **10**(4): p. 558-63.
53. Bickel, M., *The role of interleukin-8 in inflammation and mechanisms of regulation.* J Periodontol, 1993. **64**(5 Suppl): p. 456-60.
54. Yeh, M., et al., *Increased transcription of IL-8 in endothelial cells is differentially regulated by TNF-alpha and oxidized phospholipids.* Arterioscler Thromb Vasc Biol, 2001. **21**(10): p. 1585-91.
55. Clark, P.R., et al., *Increased ICAM-1 expression causes endothelial cell leakiness, cytoskeletal reorganization and junctional alterations.* J Invest Dermatol, 2007. **127**(4): p. 762-74.
56. Lawson, C. and S. Wolf, *ICAM-1 signaling in endothelial cells.* Pharmacol Rep, 2009. **61**(1): p. 22-32.
57. Frank, P.G. and M.P. Lisanti, *ICAM-1: role in inflammation and in the regulation of vascular permeability.* Am J Physiol Heart Circ Physiol, 2008. **295**(3): p. H926-H927.
58. Puhlmann, M., et al., *Interleukin-1beta induced vascular permeability is dependent on induction of endothelial tissue factor (TF) activity.* J Transl Med, 2005. **3**: p. 37.
59. Radeke, H.H., et al., *Interleukin 1-alpha and tumor necrosis factor-alpha induce oxygen radical production in mesangial cells.* Kidney Int, 1990. **37**(2): p. 767-75.
60. Zhu, H., et al., *Potent induction of total cellular and mitochondrial antioxidants and phase 2 enzymes by cruciferous sulforaphane in rat aortic smooth muscle cells: cytoprotection against oxidative and electrophilic stress.* Cardiovasc Toxicol, 2008. **8**(3): p. 115-25.
61. Corda, S., et al., *Rapid reactive oxygen species production by mitochondria in endothelial cells exposed to tumor necrosis factor-alpha is mediated by ceramide.* Am J Respir Cell Mol Biol, 2001. **24**(6): p. 762-8.
62. Kim, Y.S., et al., *TNF-induced activation of the Nox1 NADPH oxidase and its role in the induction of necrotic cell death.* Mol Cell, 2007. **26**(5): p. 675-87.
63. Panday, A., et al., *NADPH oxidases: an overview from structure to innate immunity-associated pathologies.* Cell Mol Immunol, 2015. **12**(1): p. 5-23.
64. Guan, Z., et al., *Androgen receptor (AR) signaling promotes RCC progression via increased endothelial cell proliferation and recruitment by modulating AKT --> NF-kappaB --> CXCL5 signaling.* Sci Rep, 2016. **6**: p. 37085.
65. Araujo, J.A., M. Zhang, and F. Yin, *Heme oxygenase-1, oxidation, inflammation, and atherosclerosis.* Front Pharmacol, 2012. **3**: p. 119.

66. Choi, A.M. and J. Alam, *Heme oxygenase-1: function, regulation, and implication of a novel stress-inducible protein in oxidant-induced lung injury.* Am J Respir Cell Mol Biol, 1996. **15**(1): p. 9-19.
67. Yet, S.F., et al., *Absence of heme oxygenase-1 exacerbates atherosclerotic lesion formation and vascular remodeling.* FASEB J, 2003. **17**(12): p. 1759-61.
68. Maines, M.D., *The heme oxygenase system: a regulator of second messenger gases.* Annu Rev Pharmacol Toxicol, 1997. **37**: p. 517-54.
69. Loboda, A., et al., *Heme oxygenase-1 and the vascular bed: from molecular mechanisms to therapeutic opportunities.* Antioxid Redox Signal, 2008. **10**(10): p. 1767-812.
70. Taha, H., et al., *Role of heme oxygenase-1 in human endothelial cells: lesson from the promoter allelic variants.* Arterioscler Thromb Vasc Biol, 2010. **30**(8): p. 1634-41.
71. Wardyn, J.D., A.H. Ponsford, and C.M. Sanderson, *Dissecting molecular cross-talk between Nrf2 and NF-kappaB response pathways.* Biochem Soc Trans, 2015. **43**(4): p. 621-6.
72. Loboda, A., et al., *Role of Nrf2/HO-1 system in development, oxidative stress response and diseases: an evolutionarily conserved mechanism.* Cell Mol Life Sci, 2016. **73**(17): p. 3221-47.
73. Alam, J. and J.L. Cook, *How many transcription factors does it take to turn on the heme oxygenase-1 gene?* Am J Respir Cell Mol Biol, 2007. **36**(2): p. 166-74.
74. Genlantis. *eLUCidate™ Luciferase Reporter Cell Lines*. Available from: https://lib.store.yahoo.net/lib/yhst-131428861332406/EL-NFKBRAW-elucidate.pdf.
75. Behzadi, S., et al., *Cellular uptake of nanoparticles: journey inside the cell.* Chem Soc Rev, 2017. **46**(14): p. 4218-4244.
76. Park, S., et al., *Cellular uptake pathway and drug release characteristics of drug-encapsulated glycol chitosan nanoparticles in live cells.* Microsc Res Tech, 2010. **73**(9): p. 857-65.
77. Wieth, J.O., P.J. Bjerrum, and C.L. Borders, Jr., *Irreversible inactivation of red cell chloride exchange with phenylglyoxal, and arginine-specific reagent.* J Gen Physiol, 1982. **79**(2): p. 283-312.
78. Alawdi, S.H., et al., *Loading Amlodipine on Diamond Nanoparticles: A Novel Drug Delivery System.* Nanotechnol Sci Appl, 2019. **12**: p. 47-53.
79. Zupancic, G., et al., *Differential exocytosis from human endothelial cells evoked by high intracellular Ca(2+) concentration.* J Physiol, 2002. **544**(3): p. 741-55.
80. Romero, F., et al., *Aristoteline, an Indole-Alkaloid, Induces Relaxation by Activating Potassium Channels and Blocking Calcium Channels in Isolated Rat Aorta.* Molecules, 2019. **24**(15).
81. Francia, V., et al., *Limits and challenges in using transport inhibitors to characterize how nano-sized drug carriers enter cells.* Nanomedicine (Lond), 2019. **14**(12): p. 1533-1549.

82. Koivusalo, M., et al., *Amiloride inhibits macropinocytosis by lowering submembranous pH and preventing Rac1 and Cdc42 signaling.* J Cell Biol, 2010. **188**(4): p. 547-63.
83. Roden, D.M., *Pharmacogenetics of Potassium Channel Blockers.* Card Electrophysiol Clin, 2016. **8**(2): p. 385-93.
84. Cherian, O.L., A. Menini, and A. Boccaccio, *Multiple effects of anthracene-9-carboxylic acid on the TMEM16B/anoctamin2 calcium-activated chloride channel.* Biochim Biophys Acta, 2015. **1848**(4): p. 1005-13.
85. Rouzaire-Dubois, B. and J.M. Dubois, *K+ channel block-induced mammalian neuroblastoma cell swelling: a possible mechanism to influence proliferation.* J Physiol, 1998. **510 (Pt 1)**: p. 93-102.
86. Wu, D. and P. Yotnda, *Induction and testing of hypoxia in cell culture.* J Vis Exp, 2011(54).
87. Alejandra, R., S. Natalia, and E.D. Alicia, *The blocking of aquaporin-3 (AQP3) impairs extravillous trophoblast cell migration.* Biochem Biophys Res Commun, 2018. **499**(2): p. 227-232.
88. Kjellerup, L., et al., *Identification of Antifungal H(+)-ATPase Inhibitors with Effect on Plasma Membrane Potential.* Antimicrob Agents Chemother, 2017. **61**(7).
89. Martin, D.K., et al., *Chloride ion channels are associated with adherence of lymphatic endothelial cells.* Microvasc Res, 1996. **52**(3): p. 200-9.

APPENDIX A

TABLES

Table 1. Inhibitors Used for Uptake/Release Assay. *List of channel blockers and endocytosis disruptors. Display of abbreviated name, concentrations used, and the function of the potential inhibitors.*

Inhibitor Name	*Abbrev*	*Conc.*	*Function*
4-Aminopyridine ~98%	4-AP	5mM	Ion channel blocker (K^+) [80]
Amiloride Hydrochloride Dihydrous	Amil	50uM	Inhibits micropinocytosis: blocks Na+/H+ exchanger pump [76, 81, 82]
Amiodarone Hydrochloride	Amio	10uM	Non-selective ion channel blocker [83]
Amlodipine	Aml	10uM	Ion channel blocker (Ca^+) [78]
Anthracene-9-Carboxilic Acid	Ant	100uM	Ion channel blocker (Cl^-) [84]
Barium Chloride Anhydrous	Ba	350uM	Ion channel blocker (K^+) [80]
Cesium Chloride, 99%	Cs	1mM	Ion channel blocker (K^+) [85]
Chlorpromazine HCL	Chl	10uM	Suppresses clathrin disassembly [45, 76]
Cobalt (II) Chloride	Co	2mM	Ion channel blocker (Ca^+) [86]
Copper Sulfate	Cu	100uM	hAQP3 Aquaporins [87]
Cytochalasin A	Cyt	5ug/mL	Actin disruptor [45]
Ebselen	Eb	15uM	Inhibits mammalian H^+, K^+ - ATPase [88]
Genstein	Gen	200uM	Inhibits tyrosine kinase receptors [45]
Mercury Chloride	Hg	50uM	hAQPI Aquaporins [87]
N-Phenlanthranilic Acid	N-Ph	0.1mM	Ion channel blocker (Cl^-) [89]
Niflumic Acid	Nif	10uM	Ion channel blocker (Cl^-)
Nocodazole	Noc	20uM	Actin and microtubule disruptor [45]
Phenylglyoxal	Phen	100ug	Selective inhibitor of phagocytosis [77]

APPENDIX B

FIGURES

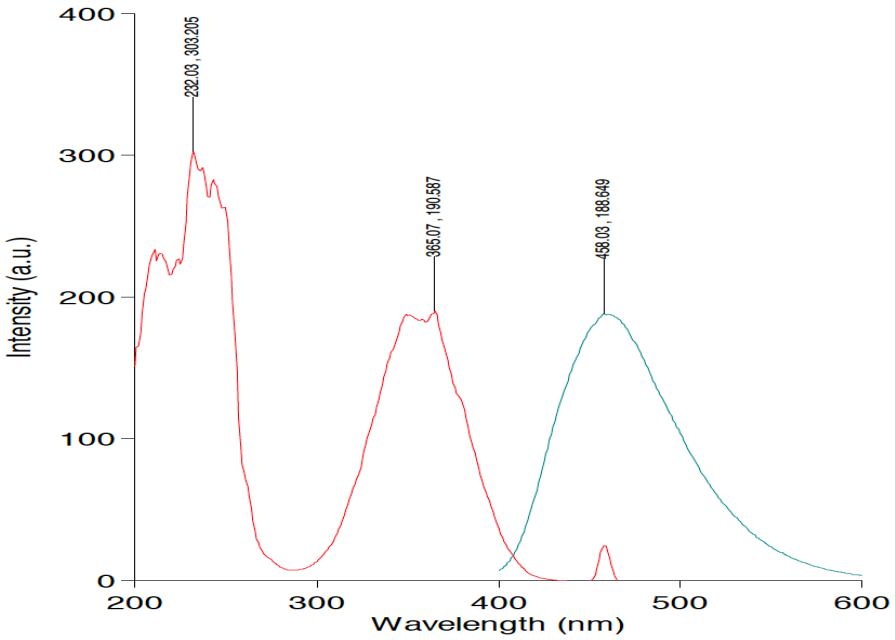

Figure 1. Characterization of CNDs. *UV-Vis photoluminescence in a.u. Measurements taken by Cary® Eclipse™ Fluoresence Spectophotometer. Excitation ranged from 300-600nm with a peak at 365nm and Emission ranged from 400-600nm with a peak at 458nm.*

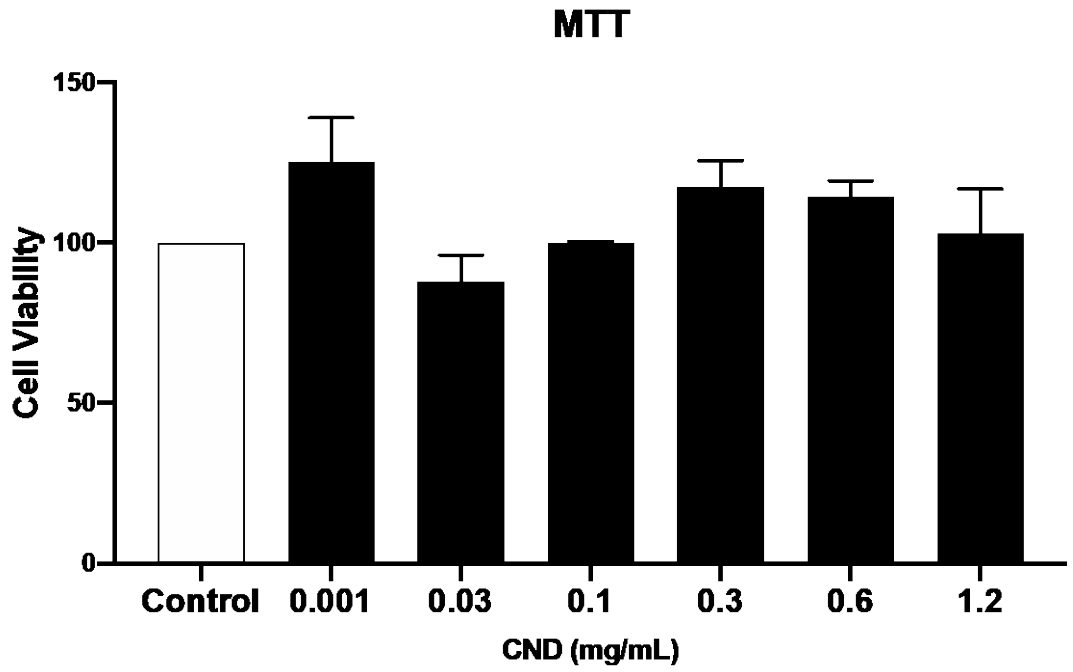

Figure 2. Cell Viability with MTT Assay. *HMEC-1 cells were treated with varying concentrations of CNDs for 6 hours. After treatment, cells were washed two times with PBS, and cells were treated with MTT dye for two hours. After tw- hour incubation, purple formazan was disolved in DMSO. Bio-Tek® Synergy plate reader was used at 570nm to determine colormetric reading. No significant change in cell viability was determined to occur. All data represent mean ± SEM. (n = 3, P > 0.05 vs. control).*

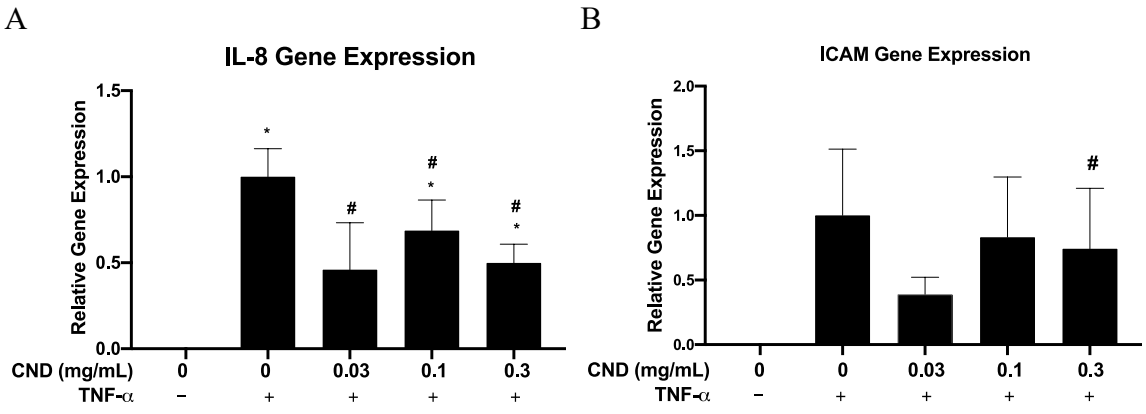

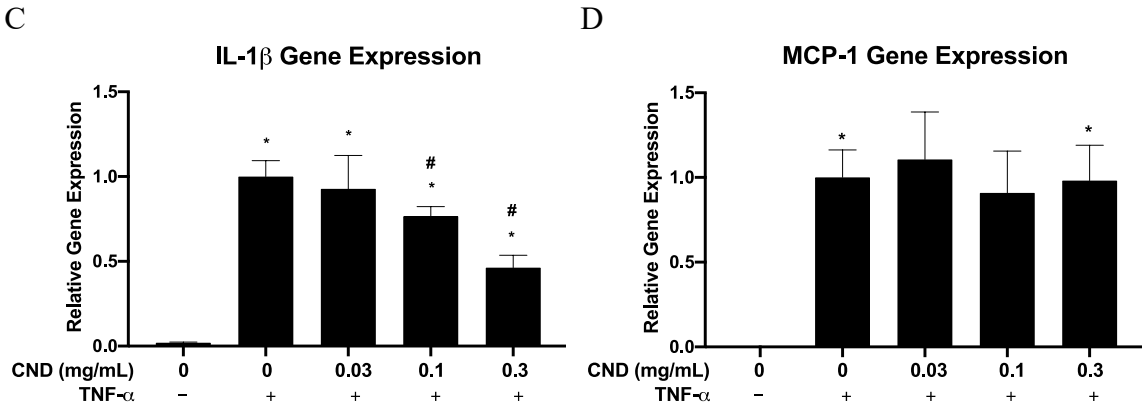

Figure 3. qRT-PCR Proinflammatory Gene Expression. *HMEC-1 cells underwent treatment with 10ng/mL of TNF-α as indicated with the presence or absence of 0.03, 0.1 or 0.3 mg/mL of CNDs for 6 hours. After treatment, cells underwent RNA extraction, cDNA synthesis and qRT-PCR. (a) IL-8, (b) ICAM, (c) IL-1β, (d) MCP-1. A significant change was demonstrated during analysis of gene expression. All data represent mean ± SEM. (n = 3-6 except for CND treatment for IL-8 and ICAM at 0.03mg/mL concentration n=2, *, P < 0.05 vs control, # P < 0.05 vs TNF-α).*

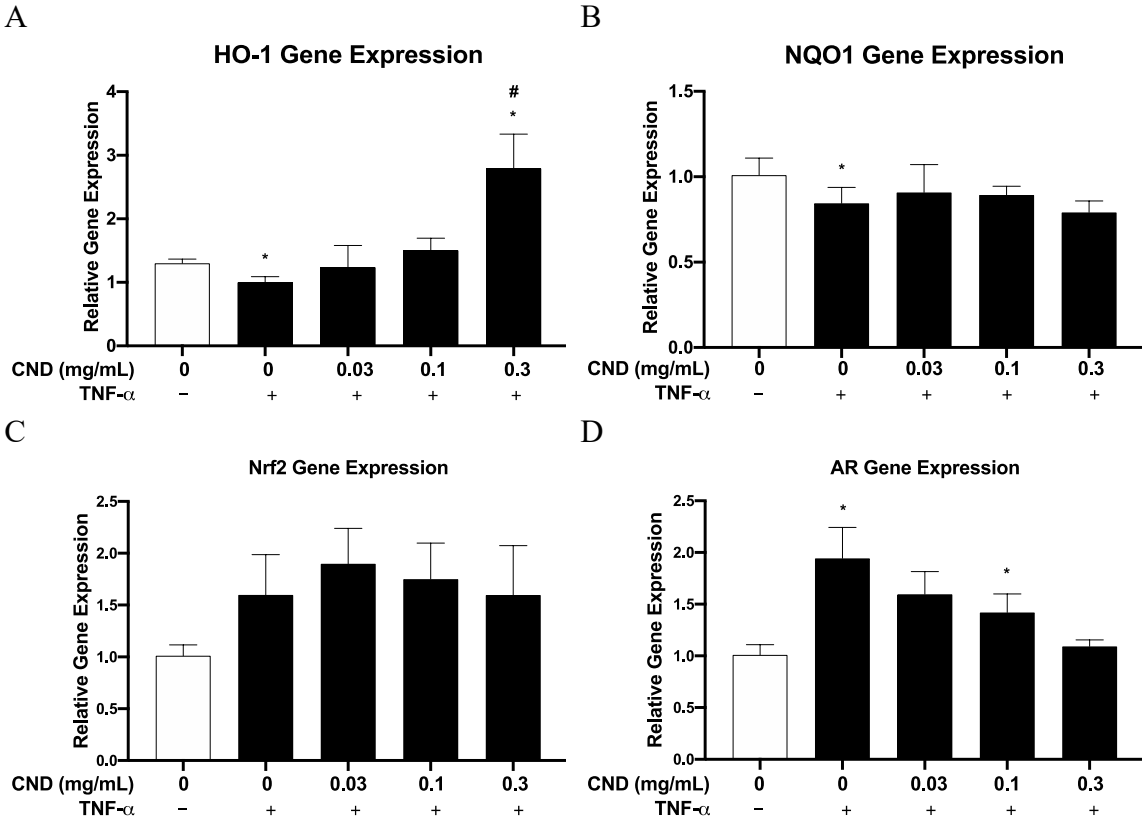

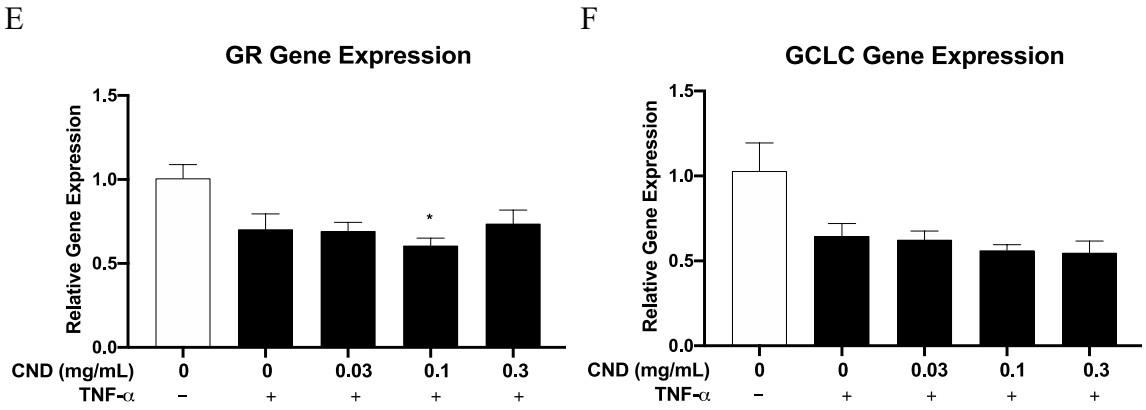

Figure 4. qRT-PCR Phase II Antioxidant Enzyme Gene Expression. *HMEC-1 cells underwent treatment with 10ng/mL of TNF-α as indicated with the presence or absence of 0.03, 0.1 or 0.3 mg/mL of CNDs for 6 hours. After treatment, cells underwent RNA extraction, cDNA synthesis and qRT-PCR. (a) HO-1, (b) NQO1, (c) Nrf2, (d) AR, (e) GR (f) GCLC. Genes displayed no significant change in expression. All data represent mean ± SEM. (n =3-6, *, P < 0.05 vs control, #, P < 0.05 vs TNF-α).*

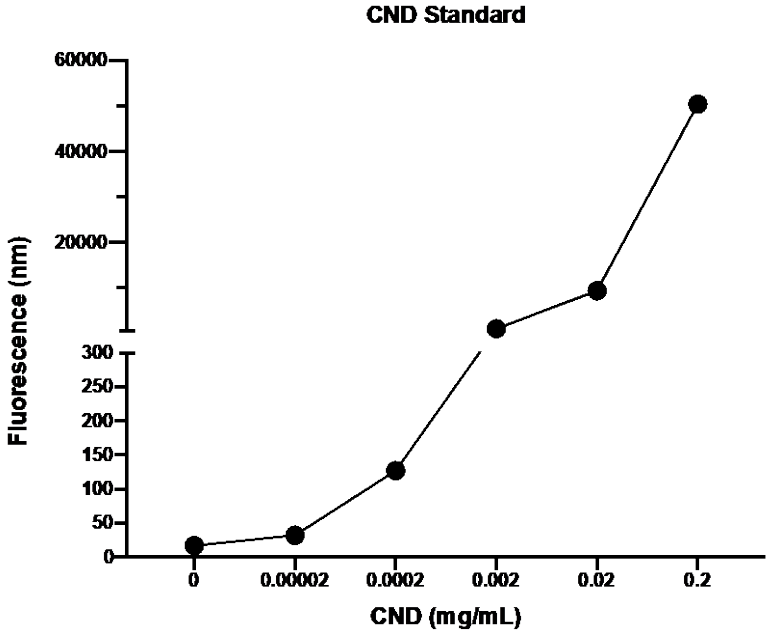

Figure 5. CND Standard. *A standard was created by completing a serial dilution of CNDS in di-water and then fluorescence was measured. Bio-Tek® Synergy plate reader was used at 360/40 excitation and 460/40 emission.*

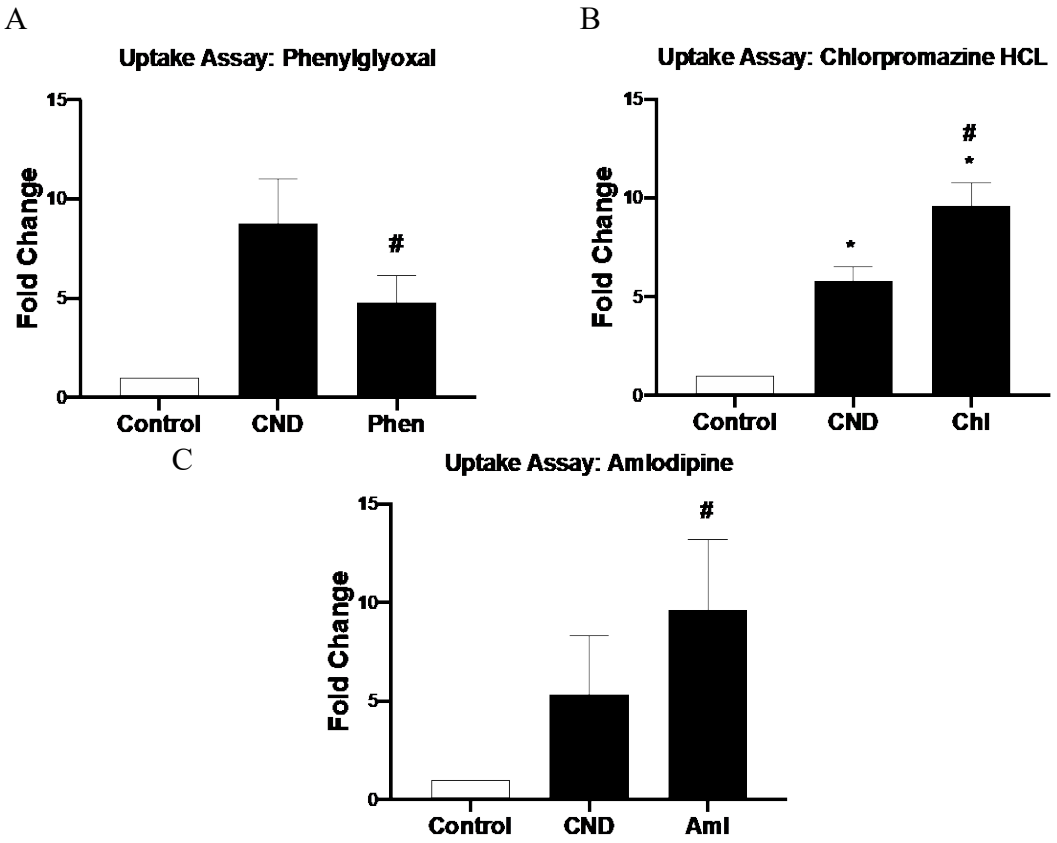

Figure 6. CND Uptake. *HMEC-1 cells were treated with inhibitors with concentrations described (Table 1) for 30 minutes. Cells were then washed two times with PBS and treated for 6 hours, with 0.1 mg/mL of CNDs. After CND treatment, cells were washed two times with PBS and removed. Cells fluorescences were checked using the Bio-Tek® Synergy plate reader at 360/40 excitation and 460/40 emission. Inhibitors displayed a significant change in fluorescent intensity during uptake analysis. All data represent mean ± SEM. (n=3, *, P < 0.05 vs. Control. #, P < 0.05 vs CND).*

A

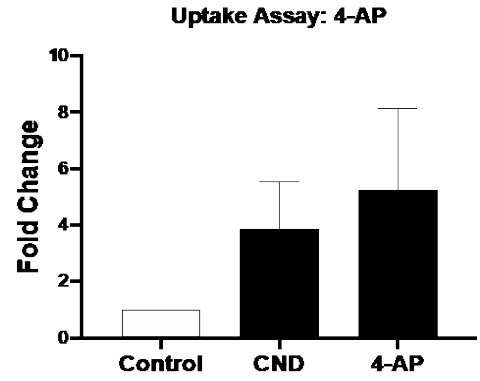
Uptake Assay: 4-AP
Fold Change
0
2
4
6
8
10
Control
CND
4-AP

B

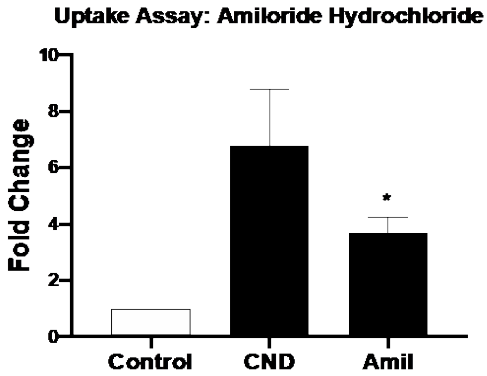
Uptake Assay: Amiloride Hydrochloride
Fold Change
0
2
4
6
8
10
*
Control
CND
Amil

C

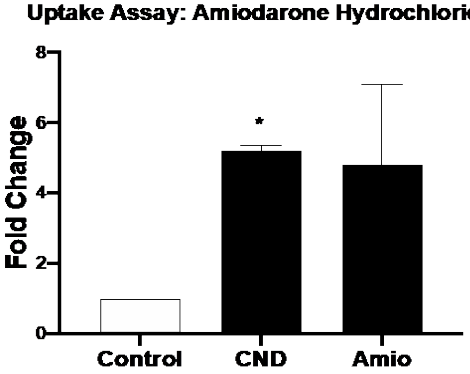
Uptake Assay: Amiodarone Hydrochloride
Fold Change
0
2
4
6
8
*
Control
CND
Amio

D

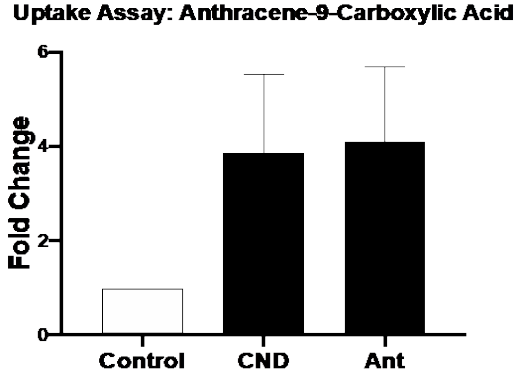
Uptake Assay: Anthracene-9-Carboxylic Acid
Fold Change
0
2
4
6
Control
CND
Ant

E

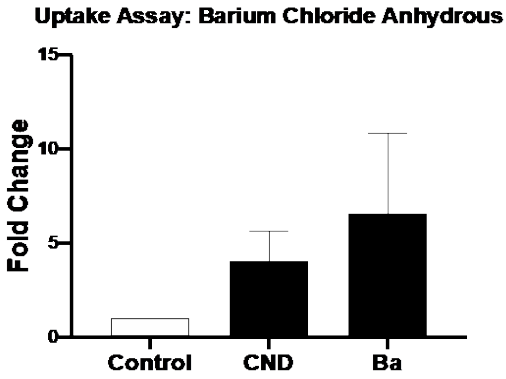
Uptake Assay: Barium Chloride Anhydrous
Fold Change
0
5
10
15
Control
CND
Ba

F

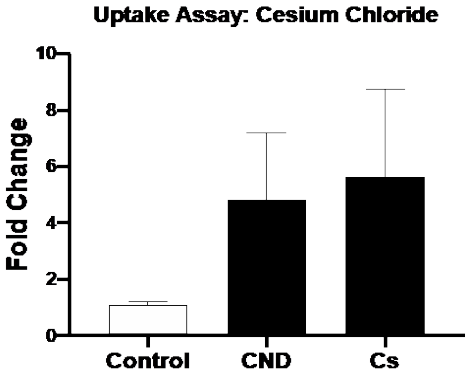
Uptake Assay: Cesium Chloride
Fold Change
0
2
4
6
8
10
Control
CND
Cs

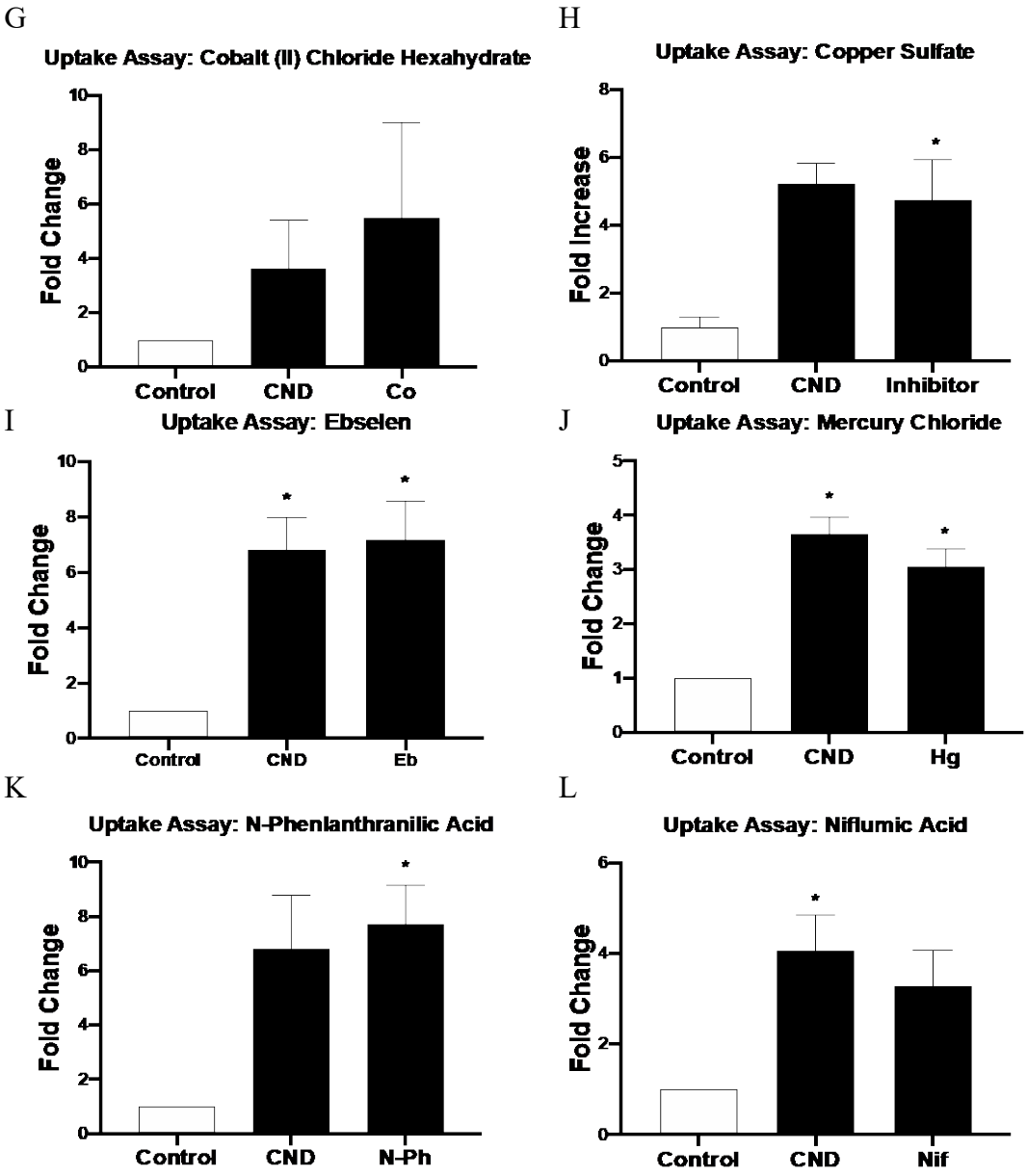

Figure 7. CND Uptake with Channel Blockers. *HMEC-1 cells were treated with inhibitors with concentrations described (Table 1), for 30 minutes. Cells were then washed two times with PBS and treated for 6 hours with 0.1 mg/mL of CNDs. After CND treatment, cells were washed two times with PBS and removed. Cells fluorescence was checked using the Bio-Tek® Synergy plate reader at 360/40 excitation and 460/40 emission. Channel blocking inhibitors displayed no significant change in fluorescent intensity. All data represent mean ± SEM. (n=3-5, *, P < 0.05 vs. Control).*

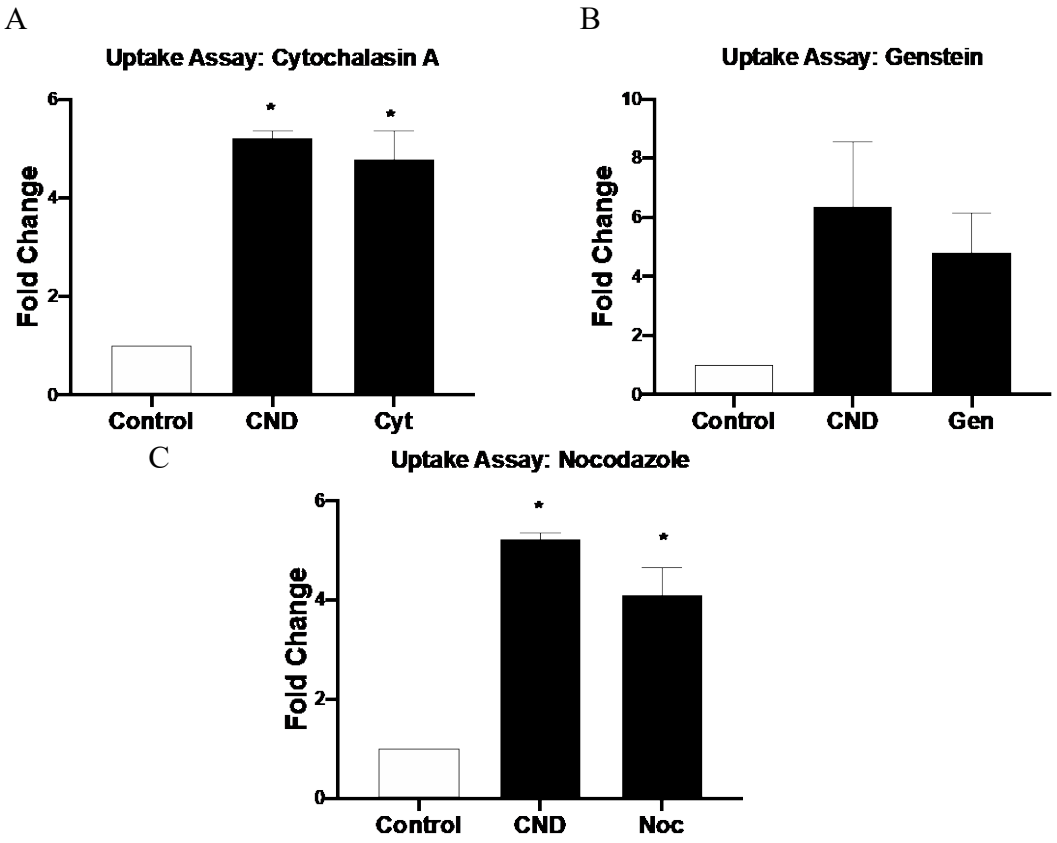

Figure 8. CND Uptake with Endocytosis Disruptor. *HMEC-1 cells were treated with inhibitors with concentrations described (Table 1), for 30 minutes. Cells were then washed two times with PBS and treated for 6 hours with 0.1 mg/mL of CNDs. After CND treatment, cells were washed two times with PBS and removed. Cells fluorescence was checked using the Bio-Tek® Synergy plate reader at 360/40 excitation and 460/40 emission. Endocytosis disruptors displayed did not show a significant change in fluorescent intensity. All data represent mean ± SEM. (n=3, *, P < 0.05 vs Control).*

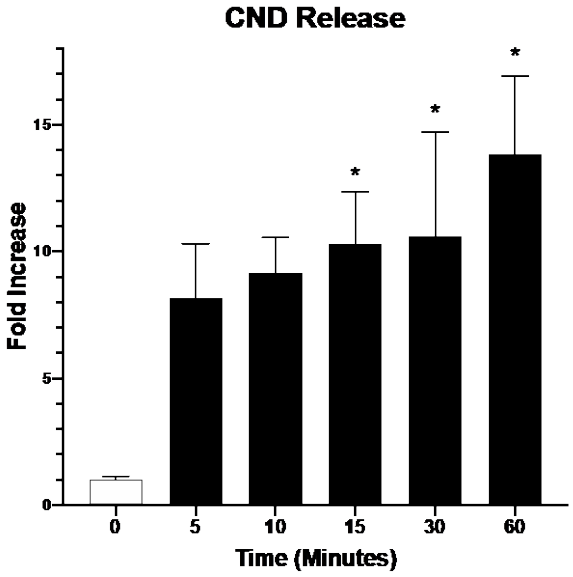

Figure 9. CND Release. *HMEC-1 cells treated with 0.1mg/mL of CNDs in HBSS for 6 hours. After treatment, cells were washed two times with PBS, and incubated in PBS for times indicated above. The supernatant was collected, spun down in a centrifuge and collected again. Fluorescence intensity of supernatant was determined by using the Bio-Tek® Synergy plate reader set at 360/40 excitation and 460/40 emission. A significant increase in fluorescence occurred at 15, 30 and 60 minutes. All data represent mean ± SEM. (n = 3, *, P < 0.05 vs. control)*

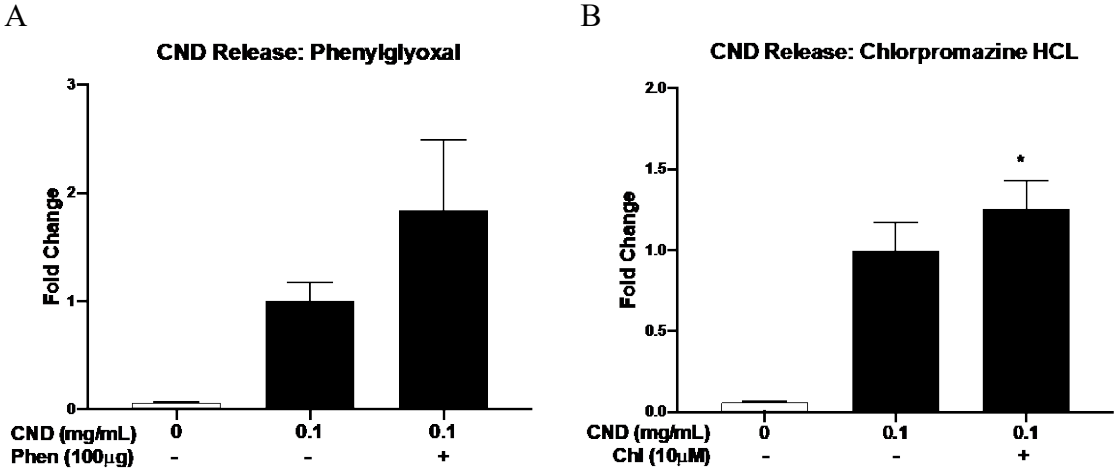

Figure 10. CND Release with Endocytosis Disruptors. *HMEC-1 cells were treated with 0.1mg/mL of CNDs for 6 hours. After treatement, cells were washed two times in PBS and incubated with either phenylglyoxal or Chlorpromazine at concentrations indicated, during 30-minute release. The supernatant was collected, spun down in a*

*centrifuge, and collected again. Fluorescence intensity of supernatant was determined by using the Bio-Tek® Synergy plate reader set at 360/40 excitation and 460/40 emission. (a) Phenylglyoxal, (b) Chlorpromazine HCL. All data represent mean ± SEM. (n = 3, *, P < 0.05 vs. CND)*

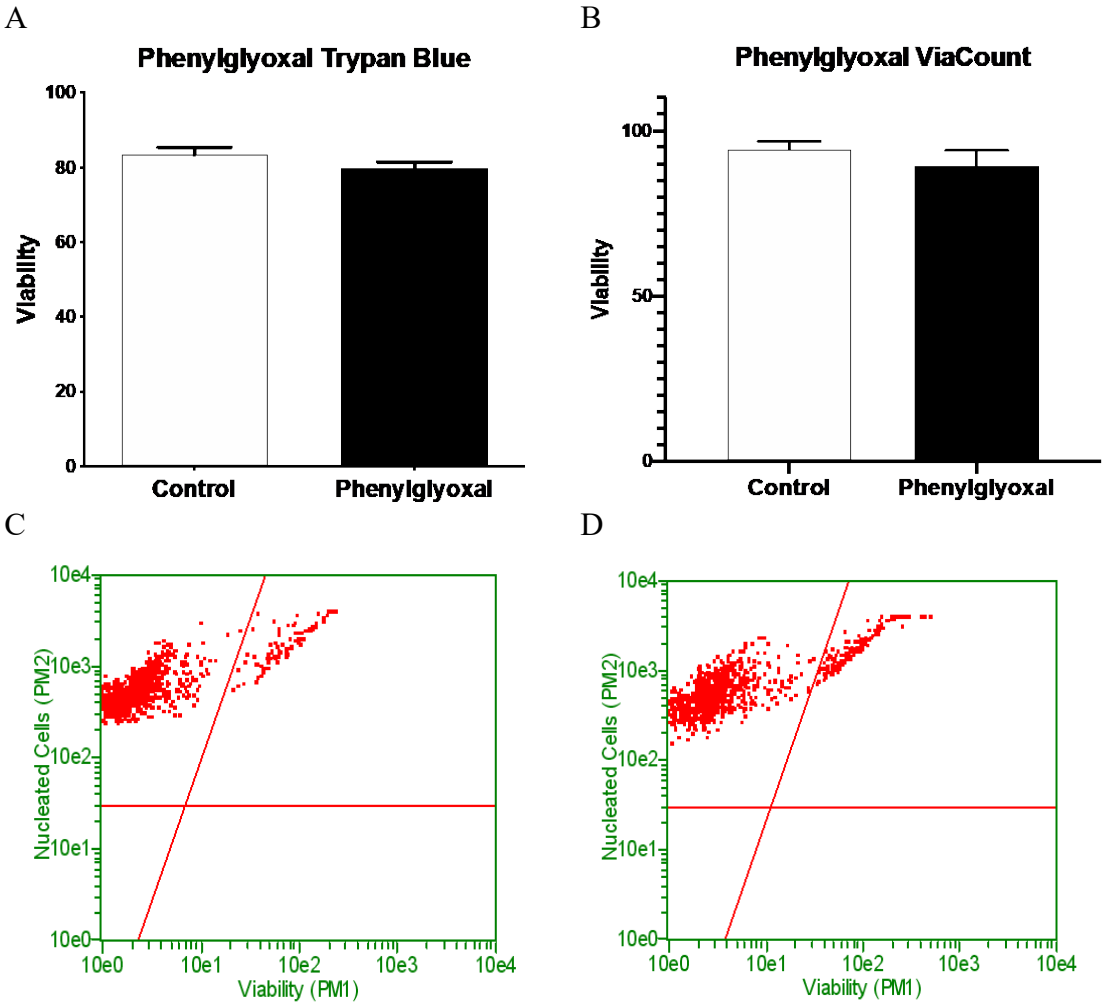

Figure 11. Cell Viability with Endocytosis Disruptor. *HMEC-1 cells were treated with 100µg of phenylglyoxal for 30 minutes. (a) HMEC-1 cells underwent 30-minute treatment with inhibitor. After treatment, cells were washed two times in PBS and incubated in HBSS for 6 hours. Cells underwent Trypan Blue viability test. (b) HMEC-1 cells underwent 30-minute treatment with inhibitor. Cells were then washed two times with PBS and underwent Viacount™ Viability test. (c) ViaCount™ Control results. (d) ViaCount™ Phenylglyoxal results. All data represent mean ± SEM. (n = 3, P > 0.05 vs. control)*

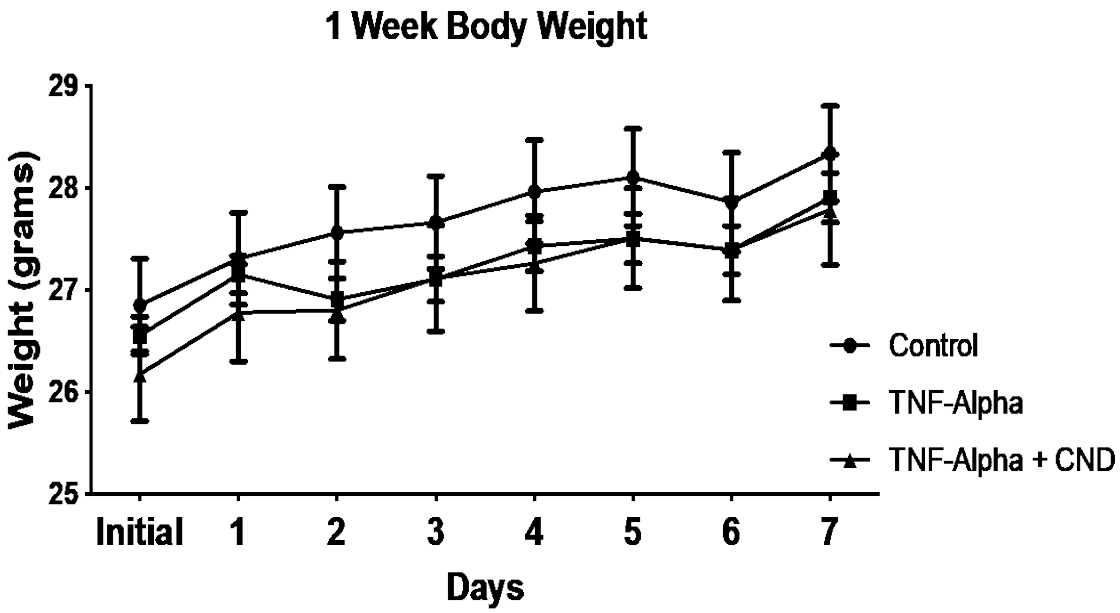

Figure 12. Animal Trial Body Weights. *Protocol 200-003. C57BL/6, male, 10-week-old mice were weighed and sorted randomly into groups on the initial day. Mice received IP injections daily beginning on day 1 and ending on day 7. Control mice received 100μL of sterile saline. TNF-Alpha group received 25μg/kg based on body weight. TNF-Alpha + CND group received 25μg/kg TNF-α + 2.5mg/kg CNDs based off body weight. No significant change in body weight was determined during the trial. (n=9-12, P > 0.05).*